Dynamic Analysis of Floating Solar Unit Subjected to Waves & Current Loadings-Numerical Modelling

by

Najmi Afiq bin Juma'at

18002906

Dissertation submitted in partial fulfilment of

The requirement for the Bachelor of Engineering (Hons)

(Civil Engineering)

JANUARY 2022

Universiti Teknologi PETRONAS,

32610 Seri Iskandar,

Perak Darul Ridzuan

CERTIFICATION OF APPROVAL

Dynamic Analysis of Floating Solar Unit Subjected to Waves & Current Loadings-Numerical Modelling

by

Najmi Afiq bin Juma'at

18002906

A project dissertation submitted to the

Civil & Environmental Engineering Programme

Universiti Teknologi PETRONAS

In partial fulfillment of the requirement for the

BACHELOR OF ENGINGEERING (Hons)

(CIVIL)

Approved by,

(Dr Ahmad Mahamad Al-Yacouby)

UNIVERSITI TEKNOLOGI PETRONAS

BANDAR SERI ISKANDAR, PERAK

JANUARY 2022

CERTIFICATION OF ORIGINALITY

This is to certify that I am responsible for the work submitted in this project, that the original work is my own except as specified in the references and acknowledgements, and the original work contained herein have not been undertaken or done by unspecified sources or person

(Najmi Afiq bin Juma’at)

ABSTRACT

The depletion of fossil fuels due to rapid global growth has led to new research and development of renewable energy. Solar Energy has become an essential form of renewable energy as part of sustainable energy. Floating solar farms or floating photovoltaics (PV) has emerged as a new development for solar energy due to no land occupancy needed as the floating solar system is installed on the water bodies whether sea or lake. Propagation of wave and current has created a dynamic response of a floating solar farm. Numerical simulations are required to summarize the complexity of the dynamic response of floating solar farms exposed to waves and currents. The numerical model is introduced by modelling and simulation using ANSYS finite element, and the dynamic response of the floating solar farms is obtained using the computational simulation method using ANSYS AQWA. This report illustrates the modelling and simulation of floating solar farms under various environmental conditions, such as regular wave, random wave, and current, in order to essentially observe the dynamic response of floating solar farms with the effects of the waves and current. As a result of the behavior of each pontoon when subjected to the effects of waves and currents, it can be determined that each pontoon has its own specialty in withstanding the highest response. The response gap between regular waves for airy wave theory and Stokes 2nd order is quite minor, whereas random waves, JONSWAP and PM spectrum have a big response difference. Finally, waves with 0 degrees have a stronger response than waves than other degrees.

ACKNOWLEDGEMENTS

First and foremost, Alhamdulillah, all praises to Allah S.W.T, I was able to complete my final year project over the course of two consecutive semesters, which I consider to be a great accomplishment. Even in the midst of the Covid-19 pandemic scenario, which has had an impact on the learning and research initiatives that have been undertaken.

I would like to thank my supervisor, Dr. Ahmad Mahamad Al-Yacouby, has always been supportive of my Final Year Project (FYP). He was a dedicated supervisor who shared his knowledge. Despite his heavy workload at university, he always made time for me. His encouragement and guidance regarding the tasks inspired me and helped me compose this report. This stage is vital for my post-graduation education journey.

At the same time, I would like to express my gratitude to his General Assistant (GA), Mr. Mostafa Mohamed Ahmed Mohamed for his continuous guidance and discussion with me. I have spent a lot of time learning this model and doing simulation.

Thank you so much to my parents and family for their unwavering support, as well as their constant encouragement, motivation, and attention. A special thank you to all of my friends who have stood by me through the highs and lows of completing the course of study.

Finally, I would want to express my gratitude to Abdul Rais bin Abdul Rashid and Mohamad Rahmad bin Alias, who were both members of my Final Year Project team and dear friends of mine. The long sleepless nights have been well worth it, as the project has been completed successfully.

TABLE OF CONTENT

FRONT PAGE		
CERTIFICATION OF APPROVAL		i
CERTIFICATION OF ORIGINALITY		ii
ABSTRACT		iii
ACKNOWLEDGEMENTS		iv
TABLE OF CONTENT		v-vi
LIST OF TABLES		vii-ix
LIST OF FIGURES		x
CHAPTER 1: INTRODUCTION		1
1.1	Background of Study	1-3
1.2	Problem Statements	4
1.3	Objectives	5
1.4	Scope of Study	5
CHAPTER 2: LITERATURE REVIEW		6
2.1	Floating Solar Farm System	6
2.1.1	Components of Floating Solar PV System	7
2.12	Advantages Floating Solar Farm in Malaysia	8
2.2	Type of Pontoon Shape	8
2.3	Classification of wave theory	9
2.4	Linear Airy Wave Theory	10
2.5	Stokes's Wave Theory	11
2.5.1	Equation of Stokes's 2nd Order	11
2.6	JONSWAP Spectrum	12
2.7	Pierson Moskovitz Spectrum (PM)	12
2.8	Diffraction Analysis	12
2.9	Hydrodynamic Response	13
2.10	Literature Review Summary	14-15
CHAPTER 3: METHODOLOGY		16
3.1	Modelling Floating Solar Farm with Different Pontoon Shape	16

	3.1.1	Geometric Modeling of Different Pontoon Shapes using Design Modeller	17-19
3.2		Hydrodynamic Analysis using ANSYS AQWA	20-21
3.3		Model Setup for Meshing	22
3.4		Currents Details in ANSYS AQWA	23
3.5		Hydrodynamic Response Analysis	24
3.6		Flowchart of the Project	25
CHAPTER 4: RESULT AND DISCUSSION			26
4.1		Simulation Description and Validation	26
4.2		Effects of Pontoon Shapes on Regular Wave Theory (Airy Waves and Stokes 2nd Order)	26
	4.2.1	Surge Response for Airy wave	27-28
	4.2.2	Surge Response for Stokes 2nd Order	29-30
	4.2.3	Heave Response for Airy Wave	31-32
	4.2.4	Heave Response for Stokes 2nd Order	33-34
	4.2.5	Pitch Response for Airy Wave	35-36
	4.2.6	Pitch Response for Stokes 2nd Order	37-38
	4.2.7	Maximum Response on Different Models on Regular Waves	39
4.3		Effects of Wave Types	40
	4.3.1	RAO Response in Regular Wave	40-41
	4.3.2	RAO Response in Irregular Wave	42-43
4.4		Effects of Wave Direction	44-46
CHAPTER 5: CONCLUSION AND RECOMMENDATION			47
5.1		Conclusion	47
5.2		Recommendation	47
REFERENCES			48
APPENDICES			50

LIST OF FIGURES

FIGURE NO.	TITLE	PAGE
FIGURE 1.1	Wave propagate on floating solar farms	1
FIGURE 1.2	Floating Solar System	2
FIGURE 1.3	ANSYS logo	3
FIGURE 1.4	Example of analysis using ANSYS AQWA	3
FIGURE 1.5	Typical pontoon used in FPV	4
FIGURE 2.1	Floating Solar	6
FIGURE 2.2	Le Méhauté Classification	9
FIGURE 2.3	Airy's Linear Wave Theory	10
FIGURE 2.4	The 6 DOF of a rigid body	13
FIGURE 3.1	Example Dimension of FPV	16
FIGURE 3.2	Rectangular pontoon	17
FIGURE 3.3	Cylindrical pontoon	18
FIGURE 3.4	Trapezoidal pontoon	19
FIGURE 3.5	PMO metocean data	20
FIGURE 3.6	Rectangular pontoon mesh	22
FIGURE 3.7	Project Flowchart	25
FIGURE 4.1	Airy wave surge response for cylindrical pontoon	27
FIGURE 4.2	Airy wave surge response for rectangular pontoon	27
FIGURE 4.3	Airy wave surge response for trapezoidal pontoon	27
FIGURE 4.4	Maximum response for surge	28

FIGURE 4.5	Stokes 2nd Order wave surge response for cylindrical pontoon	29
FIGURE 4.6	Stokes 2nd Order wave surge response for rectangular pontoon	29
FIGURE 4.7	Stokes 2nd Order wave surge response for trapezoidal pontoon	29
FIGURE 4.8	Maximum response for surge	30
FIGURE 4.9	Airy wave heave response for cylindrical pontoon	31
FIGURE 4.10	Airy wave heave response for rectangular pontoon	31
FIGURE 4.11	Airy wave heave response for trapezoidal pontoon	31
FIGURE 4.12	Maximum response for heave	32
FIGURE 4.13	Stokes 2nd Order wave heave response for cylindrical pontoon	33
FIGURE 4.14	Stokes 2nd Order wave heave response for rectangular pontoon	33
FIGURE 4.15	Stokes 2nd Order wave heave response for trapezoidal pontoon	33
FIGURE 4.16	Maximum response for heave	34
FIGURE 4.17	Airy wave pitch response for cylindrical pontoon	35
FIGURE 4.18	Airy wave pitch response for rectangular pontoon	35
FIGURE 4.19	Airy wave pitch response for trapezoidal pontoon	35
FIGURE 4.20	Maximum response for pitch	36
FIGURE 4.21	Stokes 2nd Order wave pitch response for cylindrical pontoon	37
FIGURE 4.22	Stokes 2nd Order wave pitch response for rectangular pontoon	37
FIGURE 4.23	Stokes 2nd Order wave pitch response for trapezoidal pontoon	37

FIGURE 4.24	Maximum response for pitch	38
FIGURE 4.25	Surge response in regular wave	40
FIGURE 4.26	Heave response in regular wave	40
FIGURE 4.27	Pitch response in regular wave	41
FIGURE 4.28	Surge response in irregular wave	42
FIGURE 4.29	Heave response in irregular wave	42
FIGURE 4.30	Pitch response in irregular wave	43
FIGURE 4.31	Surge response at wave direction	44
FIGURE 4.32	Heave response for different wave direction	45
FIGURE 4.33	Pitch response at wave direction	45

LIST OF TABLES

TABLE NO.	TITLE	PAGE
TABLE 2.1	Main Components Floating Solar	7
TABLE 2.2	Type of Pontoon Shape	8
TABLE 2.3	Formulas for Stokes' second-order wave theory	11
TABLE 2.4	Literature Review Summary	14
TABLE 2.5	Literature Review Summary	15
TABLE 3.1	Example Dimension of floating solar farm with rectangular pontoon	17
TABLE 3.2	Example Dimension of floating solar farm with cylindrical pontoon	18
TABLE 3.3	Example Dimension of floating solar farm with trapezoidal pontoon	19
TABLE 3.4	Overview of condition setting for each pontoon	21
TABLE 3.5	Mesh parameters for rectangular pontoon	22
TABLE 3.6	Current details for rectangular pontoon	23
TABLE 3.7	Wave details for rectangular pontoon	24
TABLE 4.1	Maximum response for surge, heave, and pitch	39
TABLE 4.2	Maximum response for surge, heave, and pitch	41
TABLE 4.3	Maximum response for surge, heave, and pitch	43
TABLE 4.4	Wave direction in Airy Wave	46
TABLE 4.5	Wave direction in Stokes 2nd Order	46

CHAPTER 1
INTRODUCTION

The fundamentals of the research study were covered in this chapter. It contains a detailed background investigation as well as a clear explanation of the problem statement and its objectives. This chapter also includes the project's scope of work.

1.1 Background of Study

The rapid growth of population in a country has demanded a huge amount of energy to distribute in a country. This energy demand can be divided into two categories; non-renewable and renewable (Muhammad-Sukki et al., 2012). Renewable energy resource such as solar energy plays a crucial part in a developing country. Therefore, due to limited land occupancy and the demand for energy resources due to increasing population growth, a floating solar farm or floating photovoltaic (FPV) is the most effective solution. According to (Kumar, Mohammed Niyaz, & Gupta, 2021), These problems can be countered by implementing floating photovoltaic systems, which save the land space and reduce the process of evaporation which saves water.

Figure 1.1 shows wave propagate on floating solar farms. The propagation of nonlinear waves/currents towards floating structures has significantly affected the offshore industry. The wave-current interaction is considered in the process of freak wave generation (Qu et al., 2020). Waves and currents are ubiquitous phenomena in offshore environments, and their interactions are an important topic in coastal engineering (Zhang, Jeng, Gao, & Zhang, 2013).

FIGURE 1.1: Wave propagate on floating solar farms

The problems faced by floating structure subjected to dynamic responses has not yet been completely solved due to the calculation of nonlinear wave being very complex. According to (Choi, Hong, & Choi, 2000), the problem is not being completely solved due to the complexity of nonlinear wave behavior which required the help of computational simulation. Several parameters use for this research paper such as wave height, wave period, water depth and wave spectrum that affect the dynamic characteristics of floating structure response to wave and current loadings.

Figure 1.2 shows an example of floating system in floating solar system. This report highlights 3 types of pontoon shapes that serve as a floating system for photovoltaic solar panels to float on bodies of water that are cylindrical, rectangular and trapezoidal pontoon shapes. A pontoon is a floating structure and has enough buoyancy to be on the water and bear a heavy burden, (Cazzaniga et al., 2018) stated the idea of floating PV modules are install on a raft with adequate buoyancy and to launch them in water in order to assemble the full platform. The structure is designed so that it can contain some panels.

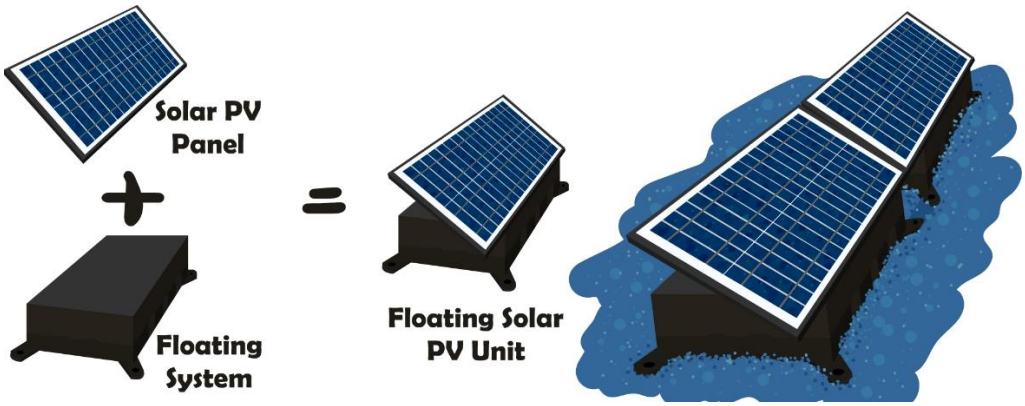

FIGURE 1.2: Floating Solar System

ANSYS Finite Element Analysis as stated in **Figure 1.3**, is a comprehensive engineering simulation software for simulating engineering structures or user-modeled components using computational methods to analyze and evaluate model performance, such as strength, hydrodynamics, and impact capabilities.

FIGURE 1.3: ANSYS logo

Figure 1.4 demonstrate an example of analysis using ANSYS AQWA. AQWA Hydrodynamic Time Response offers dynamic analysis capabilities to perform global performance evaluations of floating structures in the time domain.

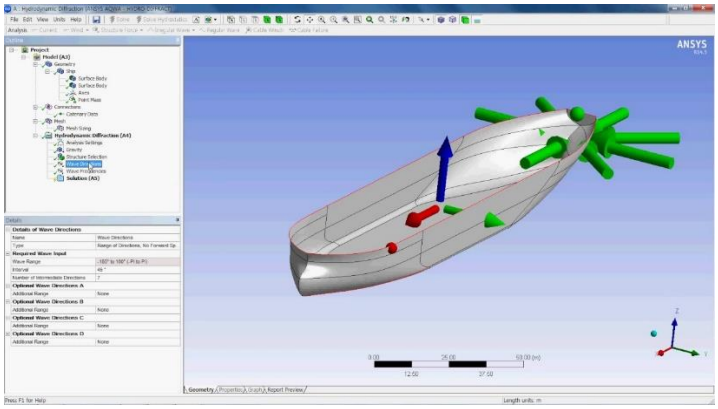

FIGURE 1.4: Example of analysis using ANSYS AQWA

1.2 Problem Statements

The floating solar system is comparatively new compared to other solar units. According to (Kaymak & Şahin, 2021), Floating solar systems are new rather than terrestrial PV system. To establish a proper floating solar system, a dynamic analysis needs to be carried out to obtain the boundary limit subjected to second-order wave and current loading that the floating solar system needs to comply with.

Figure 1.5 illustrate an example of typical pontoon used in FPV. There are various pontoon shapes used as floating systems for floating solar units. To obtain the optimum shape and size of the pontoon for the floating system, an analysis needs to be carried out to identify which pontoon shape is stable for floating solar systems. The capability to tolerate with wave force and move in motion of the wave are essential for floating solar (Kaymak & Şahin, 2021). Therefore, the design of a floating solar unit is very crucial to ensure the stability and better performance of floating solar units subject to seawater/waves. Design rules and codes of practise for both land and sea-based remote sensing systems are thought to be hindering the spread of cumulative FPV technology (Friel, Karimirad, Whittaker, Doran, & Howlin, 2019).

FIGURE 1.5: Typical pontoon used in FPV

1.3 Objectives

The objectives of this study are:

1) To conduct a parametric study on the dynamic responses of floating solar units subjected to wave and current effects.
2) To determine the effects of pontoon shape on the dynamic response of floating solar units.

Once the objectives are met, this study could potentially be a good resource for further developments of solar technology, especially in the floating solar sector.

1.4 Scope of Study

The scope of the study for this project will be to perform a dynamic analysis using ANSYS finite element modelling and simulation and ANSYS AQWA on floating solar farms with rectangular, cylinder, and trapezoidal pontoon shapes. The following are other scopes of study this project will limit itself to:

1) Conduct research on past articles and studies regarding dynamic response towards floating unit subjected to wave and current loading.
2) Create a model of floating solar unit with rectangular, cylinder, and trapezoidal floating system using ANSYS software.
3) Measure and evaluate the hydrodynamic responses subjected to second-order wave and current loading on the regular wave as controlled variables.
4) Measure and evaluate the hydrodynamic responses subjected to wave and current loading on the ocean wave with varying parameters and compare them to one another.
5) The parameters that will be the variables are the pontoon shapes, wave direction and wave spectrum.
6) To evaluate the response amplitude operator (RAO) based on the parameter's studies.

CHAPTER 2
LITERATURE REVIEW

2.1 Floating Solar Farm System

A floating solar farm is a photovoltaic (PV) system mounted on a structure that floats on surface of water such as reservoirs, dams, industrial ponds, water treatment ponds, mining ponds, lakes, and ponds. A floating solar farm is an alternative form of renewable energy source for the country that has limited land use as the installation of this floating solar farm system does not require any land space. Solar energy has risen to become one of the most widely used forms of energy in today's world. According to (Pimentel Da Silva & Branco, 2018) clean renewable energy generation is also a way to accomplish global goals such as lowering CO2 emissions to the atmosphere and avoiding extreme climate change. It is employed in a range of applications and has the potential to serve as a viable alternative to conventional energy sources (Ranjbaran, Yousefi, Gharehpetian, & Astaraei, 2019). **Figure 2.1** provides an example of floating solar farm install on surface of water.

FIGURE 2.1: Floating Solar

2.1.1 Components of Floating Solar PV System

Table 2.1 shows the main components in floating solar farms according to (Sujay, Wagh, & Shinde, 2017).

TABLE 2.1: Main Components Floating Solar

COMPONENTS	FUNCTIONS
Pontoon Structure	A structure that has enough capabilities of buoyancy to float on water bodies. The structure is designed to support heavy object to float.
Solar Panel	Known as PV panel that converts light from the sun to produce electricity. A photovoltaic system is composed of one or more solar panels combined.
Mooring system	Mooring system is a type of equipment that holds floating structure at a fix location. A mooring line connects an anchor on the seafloor to a floating structure
Solar Cable	Solar cables are specially used to outstand UV resistant and weather resistant. They can be used within a large temperature range.

2.12 Advantages Floating Solar Farm in Malaysia

Malaysia is really dependent on fossil fuels, but due to the depletion of fossil fuels, a renewable energy act have been legislated in 2011 to encourage Malaysian to be familiar with the renewable energy sector (Muhammad-Sukki et al., 2012). The rapid growth of the population in Malaysia has demanded a huge amount of energy, especially in the transport and industrial sectors. According to (Muhammad-Sukki et al., 2012) The data for transport and industry sectors is 79.9% in 2010 while residential and commercial construction is 12.8%, followed by the non-energy sector 6.5% and agriculture and forestry which is 0.8%. It is also essential to study the ocean circulation patterns since Malaysia's economy relies heavily on marine industries like commercial shipping, offshore oil operations, and fisheries (Pa'suya, Omar, Peter, & Din, 2014).

2.2 Type of Pontoon Shape

There are 3 type of pontoon shape that emphasized in this report, which is cylinder, rectangular and trapezoidal as stated in the **Table 2.2**. The purpose is to carry out which type of pontoon shape offer the most stability capabilities subjected to second-order wave and current.

TABLE 2.2: Type of Pontoon Shape

CYLINDER	RECTANGULAR	TRAPEZOIDAL

2.3 Classification of wave theory

Classification of wave theory according to Le Méhauté (1976). The classification of wave theory is shown in **Figure 2.2**. Ocean waves are, by their very nature, unpredictable. In contrast, larger waves in a random wave series may be transformed into a regular wave that can be described by a deterministic theory, and this is known as a periodic wave. These wave theories, despite their idealistic nature, are extremely beneficial in the design of offshore construction and the structural parts that support it. This section discusses the wave theories that are commonly used to design offshore constructions and how they work.

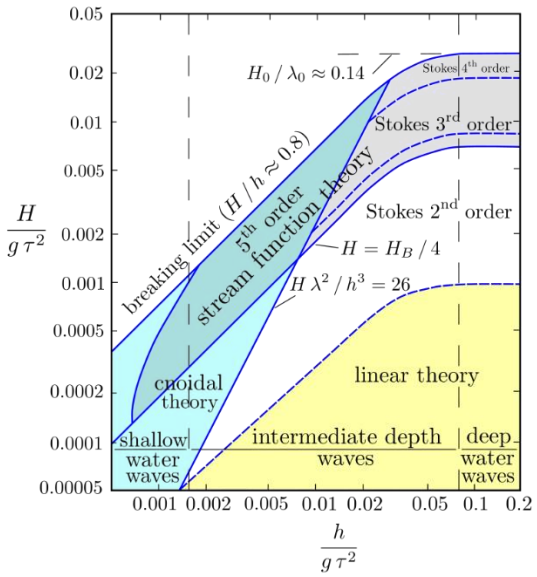

FIGURE 2.2: Le Méhauté Classification

2.4 Linear Airy Wave Theory

The airy wave theory describes a linear propagation of waves in the liquid. The assumptions of this wave theory are this theory holds a constant mean depth. This Theory is widely used in marine and coastal engineering for multiple research and test. Airy wave theory provides a rough analysis behavior of wave properties and impact. Airy wave theory describes a linear propagation of waves as shown in **Figure 2.3**:

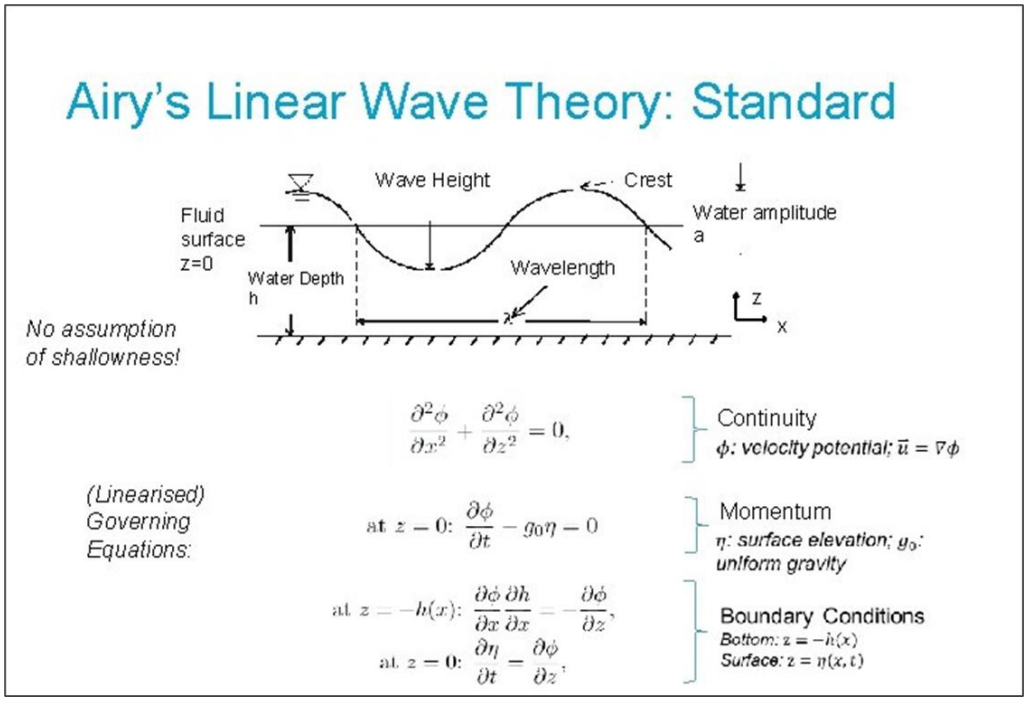

FIGURE 2.3: Airy's Linear Wave Theory

The kinematic and dynamic amplitudes are linearly proportional to the wave height according to linear theory (or wave amplitude). Hence, the normalized value is unique and invariant with respect to amplitude magnitude when these amplitudes are normalized by wave amplitude. As a function of wave period, normalized responses can be expressed as the transfer function or response amplitude operator (RAO) (Chakrabarti, 2005).

2.5. Stokes's Wave Theory

Stokes' wave theory is useful for waves in shallow and deep water. It is used to determine wave kinematics in coastal and offshore constructions. According to (Maâtoug & Ayadi, 2016) many research works are performed in the study of second-order Stokes theory. Predicting high order wave loads for a cylinder and monotower platform. The wave kinematics are then used in structural design to predict wave loads.

2.5.1 Equation of Stokes's 2nd Order

Stokes's second order is formulated as **Table 2.3** according to (Chakrabarti, 2005).

TABLE 2.3: Formulas for Stokes' second-order wave theory

Quantity	First-Order Component	Second-Order Component
Dispersion relationship	$c^2 = \frac{g}{k}\tanh kd$	$c^2 = \frac{g}{k}\tanh kd$
Wave profile	$\eta = \frac{H}{2}\cos(kx - \omega t)$	$\eta = \frac{\pi H^2}{8L}\frac{\cosh kd}{\sinh^3 kd}[2 + \cosh 2kd]\cos 2(kx - \omega t)$
Horizontal velocity	$u = \frac{\pi H}{T}\frac{\cosh ks}{\sinh kd}\cos(kx - \omega t)$	$u = \frac{3}{4c}\left(\frac{\pi H}{T}\right)^2\frac{\cosh 2ks}{\sinh^4 kd}\cos 2(kx - \omega t)$
Vertical velocity	$v = \frac{\pi H}{T}\frac{\sinh ks}{\sinh kd}\sin(kx - \omega t)$	$v = \frac{3}{4c}\left(\frac{\pi H}{T}\right)^2\frac{\sinh 2ks}{\sinh^4 kd}\sin 2(kx - \omega t)$
Horizontal acceleration	$\dot{u} = \frac{2\pi^2 H}{T^2}\frac{\cosh ks}{\sinh kd}\sin(kx - \omega t)$	$\dot{u} = \frac{3\pi}{2L}\left(\frac{\pi H}{T}\right)^2\frac{\cosh 2ks}{\sinh^4 kd}\sin 2(kx - \omega t)$
Vertical acceleration	$\dot{v} = -\frac{2\pi^2 H}{T^2}\frac{\sinh ks}{\sinh kd}\cos(kx - \omega t)$	$\dot{v} = -\frac{3\pi}{4L}\left(\frac{\pi H}{T}\right)^2\frac{\sinh 2ks}{\sinh^4 kd}\cos 2(kx - \omega t)$
Dynamic pressure	$p = \rho g\frac{H}{2}\frac{\cosh ky}{\cosh kd}\cos[k(x - ct)]$	$p = \frac{3}{4}\rho g\frac{\pi H^2}{L}\frac{1}{\sinh 2kd}\left[\frac{\cosh 2ks}{\sinh^2 kd} - \frac{1}{3}\right]\cos 2(kx - \omega t) - \frac{1}{4}\rho g\frac{\pi H^2}{L}\frac{1}{\sinh kd}[\cosh 2ks - 1]$

2.6 JONSWAP Spectrum

Models commonly use the spectral density function to describe the sea surface. Ocean wave spectral density functions have been created in a variety of ways, with the JONSWAP spectra being one of the more notable (Grainger, Sykulski, Jonathan, & Ewans, 2021). This is the fundamental equation for JONSWAP Spectrum.

$$E_{PM}(f) = \frac{\alpha g^2}{(2\pi)^4 f^5} \exp\left[-\frac{5}{4}\left(\frac{f}{f_p}\right)^{-4}\right] \gamma^{\exp\left[-\frac{(f-f_p)^2}{2\sigma^2 f_p}\right]}$$

Where,

γ = 3.30

τa = 0.07 $for\ f \leq f0$

τb = 0.09 $for\ f > f0$

α = 0.0081

2.7 Pierson Moskovitz Spectrum (PM)

This is the fundamental equation for PM Spectrum.

$$S(f) = \frac{\alpha g^2}{(2\pi)^4 f^5}\ exp[-1.25\ [\frac{\text{fo}}{\text{f}}]^4]$$

where α=0.0081and f_0=$1/Tp$

2.8 Diffraction Analysis

AQWA Hydrodynamic Diffraction demonstrates a solution for complex motion and response analysis. Computation of the second-order wave forces through the overall quadratic feature matrices allows use over an extensive variety of water depths.

2.9 Hydrodynamic Response

AQWA Hydrodynamic Time Response shows a dynamic evaluation ability for the complex assessment of floating systems within the time domain. Once a hydrodynamic solution has been done, you may see the centres of buoyancy, flotation, and gravity in the graphical display, as well as slow-drift effects and extreme-wave situations. The ANSYS AQWA simulation programme is used to calculate the dynamic reactions of floating structures. It is a suite of engineering analysis tools developed by ANSYS for the investigation of the effects of wave, wind or current on floating and fixed offshore structures like spars, floating production storage (FPSO), semi-submersible, tension leg platforms, ships and renewable energy systems and breakwater design. Station keeping and rotational vibration control at sea are crucial for ensuring the dynamic stability of floating offshore structure (Cho, Cho, Jeong, Hong, & Chun, 2013).

A stiff body has six degrees of freedom (DOF) of motion in three-dimensional space. It is possible for the body to move in three directions perpendicular to the axes on which it is oriented, including forward and backward known as surge, up and down which is heave, and left and right which is sway, as well as rotation about three perpendicular axes, which are commonly referred to as yaw (normal axis), pitch (transverse axis), and roll (rolling) (longitudinal axis). **Figure 2.4** illustrates the 6 DOF of a rigid body.

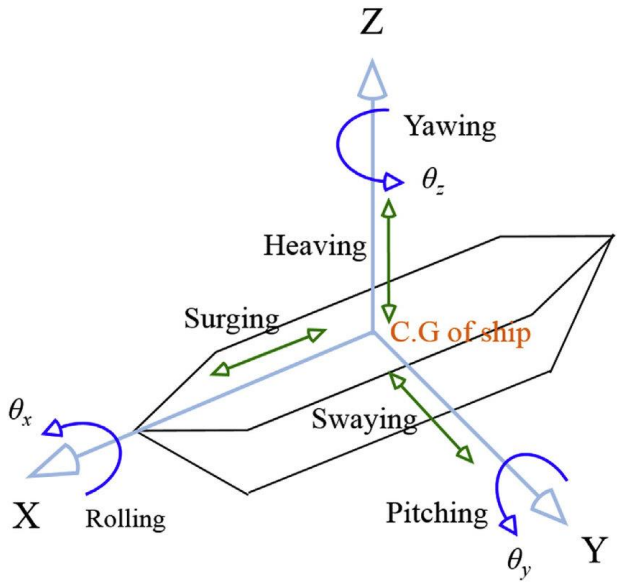

FIGURE 2.4: The 6 DOF of a rigid body

2.10 Literature Review Summary

Table 2.4 and **Table 2.5** shows the literature review summary used in this research paper.

TABLE 2.4: Literature Review Summary

No.	Author & Year	Country	Tittle	Research Gab
1.	(Sujay et al., 2017)	India	A Review on Floating Solar Photovoltaic Power Plants	This paper focus on review of various floating PV system in the world and floating PV component while this thesis focus on PMO area.
2.	(Bei, Yuan, Yu, Zhu, & Cao, 2021)	China	Numerical analysis report on fluids in floating photovoltaic power plants	This paper focus on modelling and simulation work for floating PV on 14 working conditions with different wind directions and wind speeds while this thesis focus on RAO on different pontoon shape.
3.	(Kaymak & Şahin, 2021)	Turkey	Problems encountered with floating photovoltaic systems under real conditions: A new FPV concept and novel solutions	This paper focus on experimental of three different floating PV systems with different output while this thesis focus on RAO on different pontoon shape.

TABLE 2.5: Literature Review Summary

No.	Author & Year	Country	Tittle	Research Gab
4.	(Miao, Chen, Ye, Ding, & Huang, 2021)	China	Numerical modelling and dynamic analysis of a floating bridge subjected to wave, current and moving loads	This paper focus on a numerical simulation method for calculating the dynamic properties of a floating bridge under the wave, current, and moving loads while this thesis focus floating solar farm.
5.	(Kumar et al., 2021)	India	Challenges and opportunities towards the development of floating photovoltaic systems	This paper shows an overview of various design and construction strategies with the status of FPV systems while this thesis focus on different pontoon shape as part of FPV systems.
6.	(Muhammad-Sukki et al., 2012)	Malaysia	Solar photovoltaic in Malaysia: The way forward	This paper examines solar photovoltaic (PV) in Malaysia while this thesis focus PMO metocean as parameter.
7.	(Maâtoug & Ayadi, 2016)	Tunisia	Numerical simulation of the second-order Stokes theory using finite difference method	This paper deals with computation of the second-order Stokes theory while this thesis focus on 4 different wave to analyse.

CHAPTER 3
METHODOLOGY

3.1 Modelling Floating Solar Farm with Different Pontoon Shape

It is necessary to develop the floating solar farm with different pontoon shapes in ANSYS finite element modelling and simulation software in order to perform the dynamic analysis using ANSYS AQWA finite element software. The floating solar farm with different pontoon shapes which is rectangular, cylindrical and trapezoidal are developed in the design modeler in ANSYS finite element modeling and simulation. The geometry for the floating solar farm model was derived from a research article written by (Bei et al., 2021) as a benchmark which shown in **Figure 3.1**.

2. Geometric modelling

Table 1. Geometric modeling dimensions

parts	size
Floating	1035mm*860mm*220mm
subassembly	1650mm*990mm*40mm
North-south spacing of floats	350mm
Floating east-west spacing	860mm
The angle between the component and the float	12 degrees
The surface height of the float	100mm

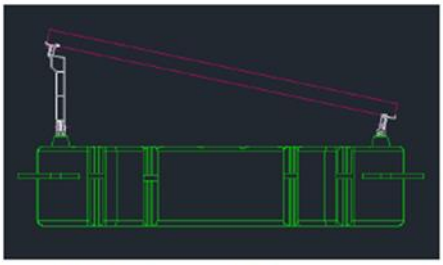

Figure 1. Side diagram of a floating power station

FIGURE 3.1: Example Dimension of FPV

3.1.1 Geometric Modeling of Different Pontoon Shapes using Design Modeller

This figure shows a rectangular pontoon for a floating solar farm. The dimensions of the solar panels, as well as the height of the column supporting the solar panels, and the diameter of the column are all fixed for three different pontoon shapes shown in **Figure 3.2**. The dimension of base pontoon (floating structure) are kept different which serves as the variables for this thesis. The geometry of the floating structure depicted in **Table 3.1**.

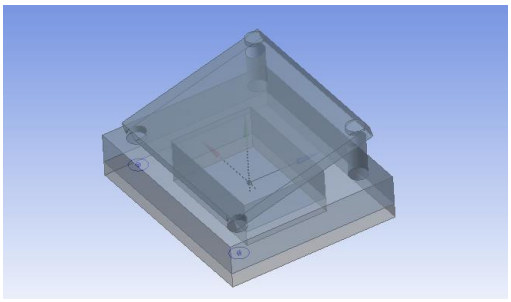

FIGURE 3.2: Rectangular pontoon

TABLE 3.1: Example Dimension of floating solar farm with rectangular pontoon

Parts	Size
Floating Structure	1035 mm * 860 mm * 220 mm
Solar Panel	754 mm * 905 mm * 60 mm
Radius of Column	45 mm
The angle between the component and the float	12 degrees
The surface height of the float	75 mm

A cylindrical pontoon for a floating solar farm is shown. The dimensions of the solar panels, the height of the solar panel support column, and the column diameter are all fixed for the three pontoon designs depicted in **Figure 3.3**. The basic pontoon (floating construction) dimensions are kept flexible for this thesis. **Table 3.2** shows the floating structure's geometry.

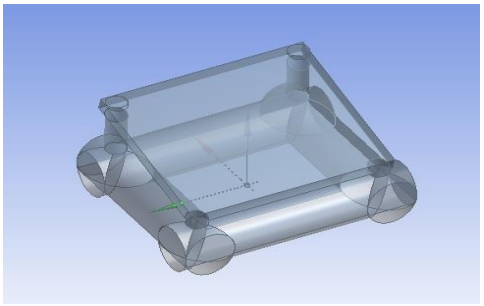

FIGURE 3.3: Cylindrical pontoon

TABLE 3.2: Example Dimension of floating solar farm with cylindrical pontoon

Parts	**Size**
Floating	V1: 1035 mm * 110^2 mm * π V2: 860 mm * 110^2 mm * π
Solar Panel	754 mm * 905 mm * 60 mm
Radius of Column	45 mm
The angle between the component and the float	12 degrees
The surface height of the float	75 mm

A trapezoidal pontoon for a floating solar farm is shown here. The size of the solar panels, the height of column that support the solar panel, and the column diameter are all fixed for the three pontoon designs indicated in **Figure 3.4**. The foundation pontoon (floating construction) dimensions are kept varied for this thesis. **Table 3.3** presents the geometry of the floating structure.

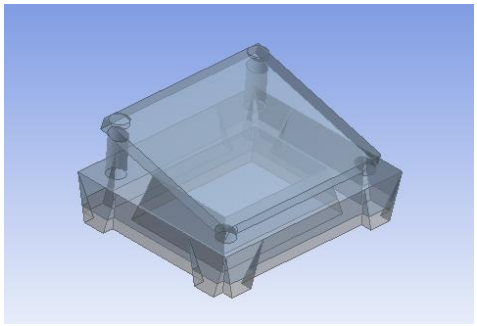

FIGURE 3.4: Trapezoidal pontoon

TABLE 3.3: Example Dimension of floating solar farm with trapezoidal pontoon

Parts	**Size**
Floating	V1: ½ * (110 mm + 220 mm) * 220 mm * 1035 mm V2: ½ * (110 mm + 220 mm) * 220 mm * 860 mm
Solar Panel	754 mm * 905 mm * 60 mm
Radius of Column	45 mm
The angle between the component and the float	12 degrees
The surface height of the float	75 mm

3.2 Hydrodynamic Analysis using ANSYS AQWA

The dynamic analysis for each structure will be tested using ANSYS AQWA to compare and analyze the response for each type of solar floating farm structure subjected to waves and currents. The simulation result is validated by comparing it to three various pontoon shapes and determining the model's optimal hydrodynamic response. The purpose of this thesis is to undertake a parametric analysis of the dynamic responses of floating solar units when subjected to waves and currents effects, as well as to determine the effect of pontoon shape on the dynamic response of floating solar units. The wave height, wave period, water depth and currents are refer to **Figure 3.5** as the guideline when setting the condition for each floating solar farms with different pontoon shapes.

L.1.1 Peninsular Malaysia Operation (PMO) (Water depth 70m)
(Note: The criteria in table below is considered as the extreme among all the sites in PMO)

Parameters	Units	Operating Criteria	100-year Storm Event
WIND			
1-min mean	m/s	20	29
3-sec Gust	m/s	22	33
WAVE [1)]			
H_s	m	4.38 [1)]	5.77
T_z	sec	6.91	8.06
T_p	sec	9.74	11.37
H_{max}	m	8.44	11.65
T_{ass}	sec	8.38	9.64
OCEAN CURRENT			
At Surface	m/s	1.24	1.67
At Mid-depth 0.5*D	m/s	0.98	1.33
At near seabed 0.01*D	m/s	0.27	0.36

FIGURE 3.5: PMO metocean data

By using floating solar farms with different pontoon shapes in 70 meters depth at the Peninsular Malaysia Operation (PMO). The wave height, wave periods, current, and frequency of waves are constant and fixed. Four waves were highlighted in this thesis which are Airy wave, Stokes 2nd order, JONSWAP spectrum, and PM spectrum which follow the PMO metocean data as stated in the **Table 3.4**. In ANSYS AQWA, Stokes 2nd Order and Airy wave theory are classified as regular wave while JONSWAP spectrum and PM Spectrum both are classified as irregular wave.

TABLE 3.4: Overview of condition setting for each pontoon

Regular wave (Airy wave, Stokes 2nd Order)	
Wave Height	8.44m
Period	8.38s
Irregular wave (JONSWAP and PM spectrum)	
Wave Height	4.38m
Period	6.91s
Gamma	3.3
Peak Frequency	1/9.74 = 0.1027Hz
Current	
Surface	1.24m/s

Since there are some limitations when choosing the wave height for regular wave, which was planned to be 8.44m, but in ANSYS AQWA, the highest wave height that can be run by the programme is 7.82m, this was the best option.

3.3 Model Setup for Meshing

The meshing capabilities of ANSYS let users save effort and time. Through the design and automating of meshing tools, ANSYS is able to assist users save simulation time. In order to obtain a more accurate outcome, the meshing of the model must be small to get a more accurate result and meshed to a suitable mesh size. **Figure 3.6** shows an example of meshing for floating solar farm with a rectangular pontoon.

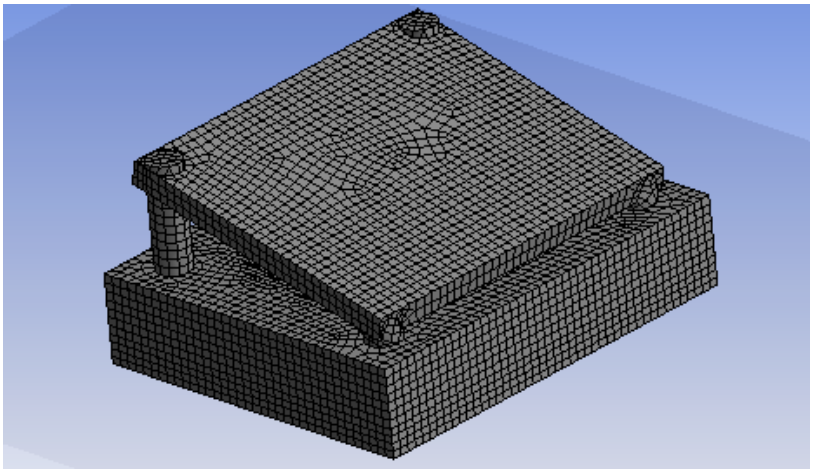

FIGURE 3.6: Rectangular pontoon mesh

Table 3.5 describes the mesh parameters for floating solar farm with rectangular pontoon shape. The meshing for both trapezoidal and cylindrical pontoons have the same value of maximum allowed frequency.

TABLE 3.5: Mesh parameters for rectangular pontoon

Mesh Parameters	
Defeaturing Tolerance	0.02 m
Maximum Element Size	0.04 m
Maximum Allowed Frequency	3.052 Hz
Meshing Type	Program Controlled
Generated Mesh Information	
Total Nodes	10294
Total Elements	10316

3.4 Currents Details in ANSYS AQWA

The type of current used is constant velocity. The speed of current is 1.24 m/s on surface of water. **Table 3.6** shows an example of current details used in this thesis.

TABLE 3.6: Current details for rectangular pontoon

Name	*Current 1*
State	Fully Defined
Details of Current 1	
Visibility	Visible
Activity	Not Suppressed
Water Depth Definition	Use Water Depth in Environment Constants
Water Depth	70 m
Current Definition	
Type	Constant Velocity
Speed	1.24 m/s
Direction	0.0°

3.5 Hydrodynamic Response Analysis

Next a hydrodynamic response analysis is performed. During this step, the response of the each pontoon shapes will be analyzed. Upon completion, the hydrodynamic time response analysis is performed. The analysis is performed using a wave height of 7.82m and a period of 8.38s as mentioned in **Table 3.4** for regular wave. **Table 3.7** presents an example of wave details of Airy wave theory. The data from **Table 3.4** are placed in the wave definition and run the simulation to obtain the results. The steps repeated for every different condition by changing the wave types and wave details for each conditions.

TABLE 3.7: Wave details for rectangular pontoon

Name	*Airy wave*
State	Suppressed
Details of Airy wave	
Visibility	Not Visible
Activity	Suppressed
Wave Definition	
Wave Type	Airy Wave Theory
Direction	0.0°
Amplitude	7.82 m
Period	8.38 s
Frequency	0.119331742243437 Hz
Ramping Method	Program Controlled

3.6 Flowchart of the Project

Figure 3.7 shows the flowchart of the project from starts to the end of this thesis.

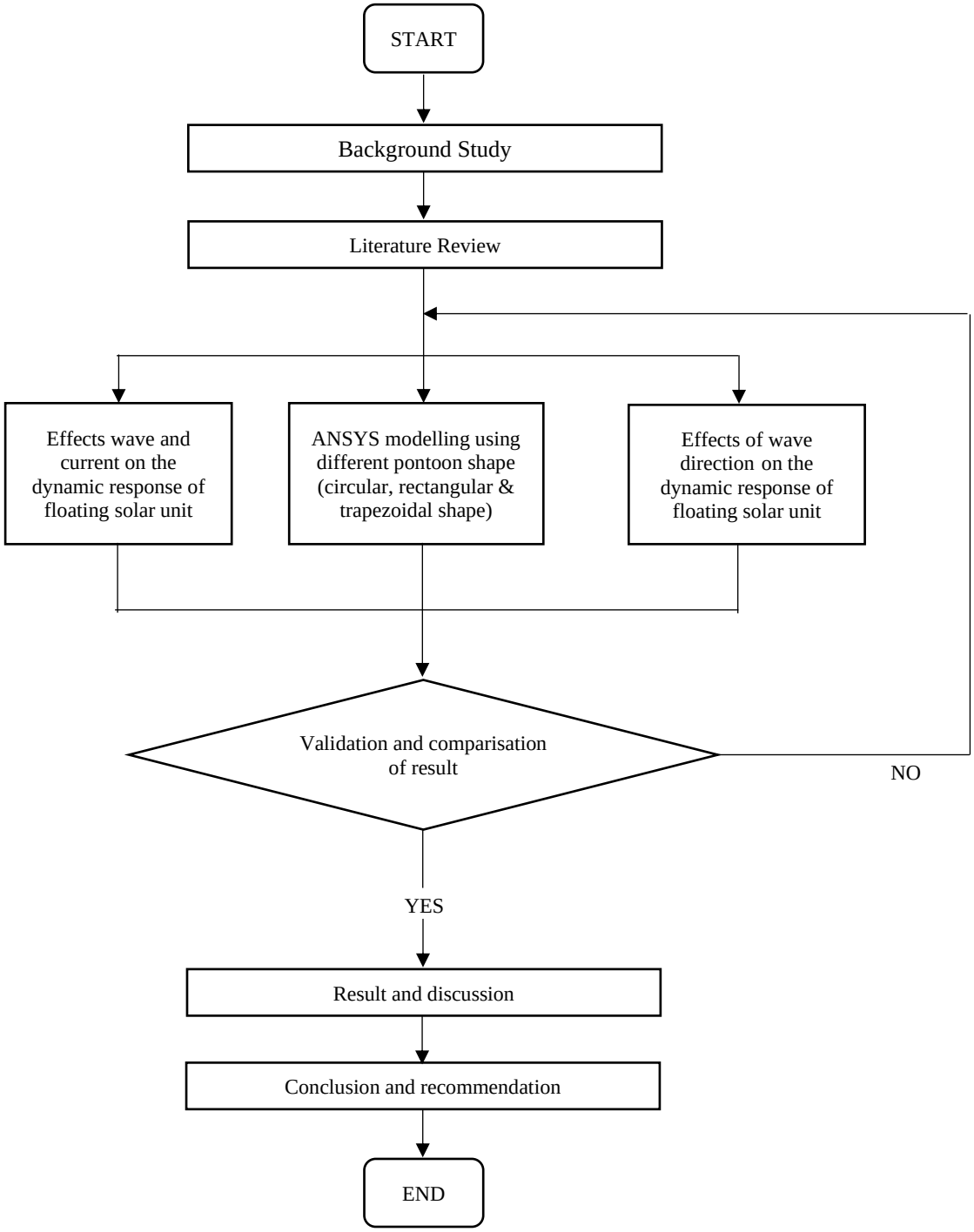

FIGURE 3.7: Project Flowchart

CHAPTER 4
RESULT AND DISCUSSION

4.1 Simulation Description and Validation

The floating solar farm model is exposed to three simulations, which are based on the environmental loadings and other characteristics:

Simulation 1: Effects of pontoon shapes on regular wave theory
Simulation 2: Effects of wave types (regular and irregular waves)
Simulation 3: Effects of wave direction

The result for Response Amplitude Operator (RAO) for each Degree of Freedom (DOF) is automatically calculated and the response will be compared under RAO-based response for three different models.

4.2 Effects of Pontoon Shapes on Regular Wave Theory (Airy Waves and Stokes 2nd Order)

The effects of different types of models were carried out to determine the maximum response for each pontoon shape's behavior when subjected to regular waves. Wave height of 7.82m, wave period of 8.38s, wave frequency of 0.119Hz, currents (constant velocity) of 1.24m/s, and wave direction of 0° were set for both Airy Waves and Stokes 2nd Order that was categorized as regular waves in ANSYS AQWA. Surge, heave, and pitch are the three DOFs highlighted in this thesis. Surge, heave and pitch were emphasized in this report due to the estimated eigenperiods are in good agreement with the experimental results in the directions of surge, heave, and pitch (Ishihara, Phuc, & Sukegawa, 2007). The responses were compared to see how each model behaved when exposed to a regular wave.

4.2.1 Surge Response for Airy wave

Figures 4.1, 4.2, and 4.3 depicted the **RAO-based response** surge for each different model under Airy Wave Theory.

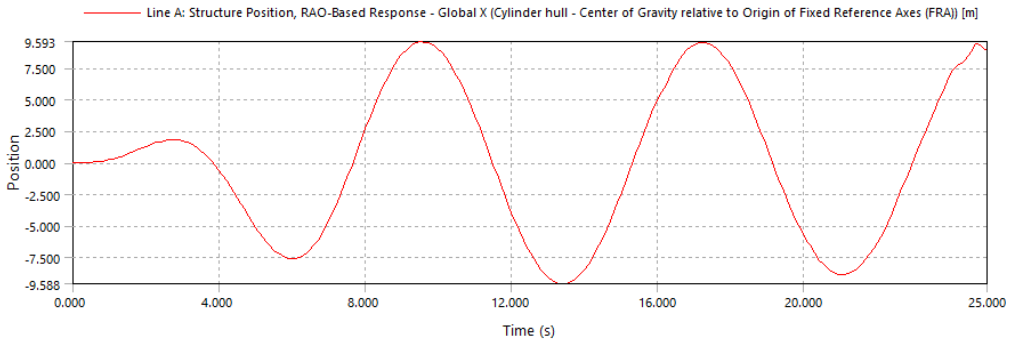

FIGURE 4.1: Airy wave surge response for cylindrical pontoon

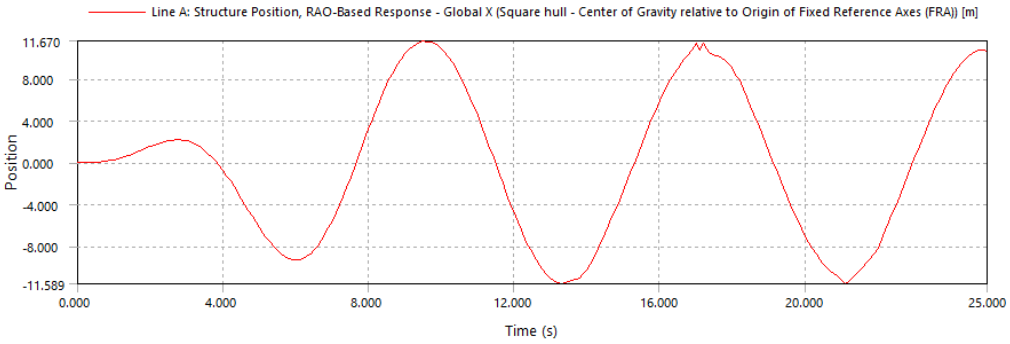

FIGURE 4.2: Airy wave surge response for rectangular pontoon

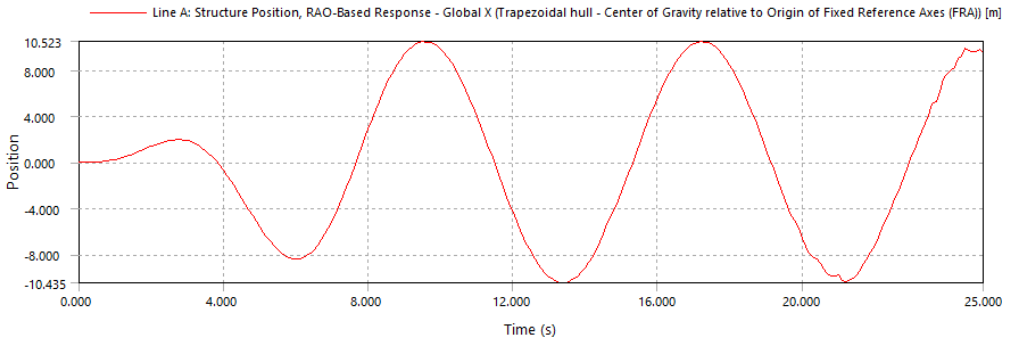

FIGURE 4.3: Airy wave surge response for trapezoidal pontoon

Figure 4.4 represents the impact of surge response on the pontoon shapes of the floating solar unit. The maximum response for the surge is the rectangular pontoon which is 11.67 m, followed by the Trapezoidal pontoon at 10.523 m and the cylindrical pontoon at 9.593 m. When comparing the three models, it is clear that the rectangular pontoon has the largest maximum response and the cylindrical pontoon has the best surge response since it has the smallest response.

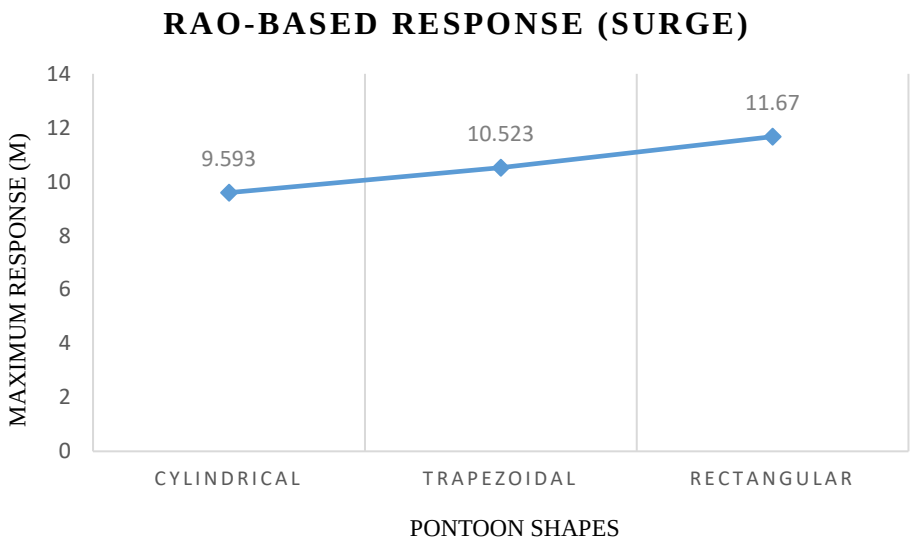

FIGURE 4.4: Maximum response for surge

4.2.2 Surge Response for Stokes 2nd Order

Figures 4.5, 4.6, and 4.7 show the characteristic of **RAO-based response** surges for different pontoons when subjected to Stokes 2nd Order wave Theory.

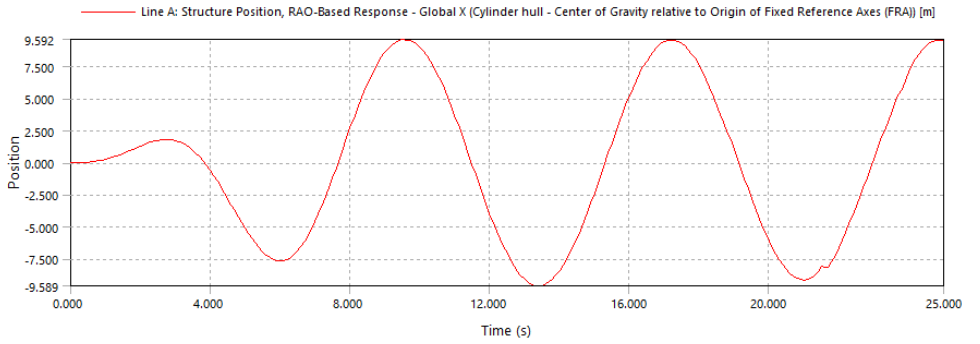

FIGURE 4.5: Stokes 2nd Order wave surge response for cylindrical pontoon

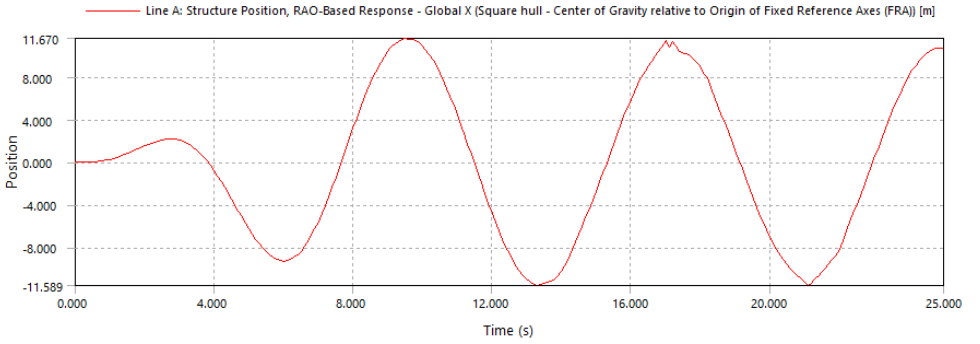

FIGURE 4.6: Stokes 2nd Order wave surge response for rectangular pontoon

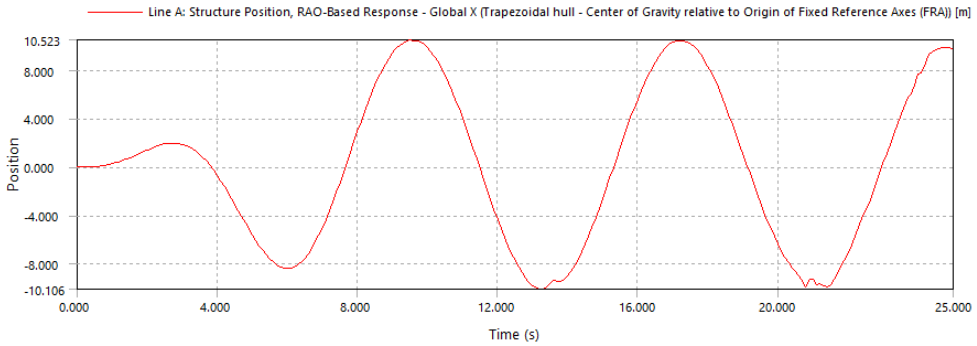

FIGURE 4.7: Stokes 2nd Order wave surge response for trapezoidal pontoon

Figure 4.8 represents the impact of surge response on the pontoon shapes of the floating solar unit. The maximum response for the surge is the rectangular pontoon which is 11.67 m, followed by the Trapezoidal pontoon at 10.523 m and the cylindrical pontoon at 9.593 m. When comparing the three models, it is clear that the rectangular pontoon has the largest maximum response and the cylindrical pontoon has the best surge response since it has the smallest response. From Airy wave and Stokes 2nd Order wave, both waves show that cylindrical pontoon is the optimal design for floating solar farms to withstand surge response.

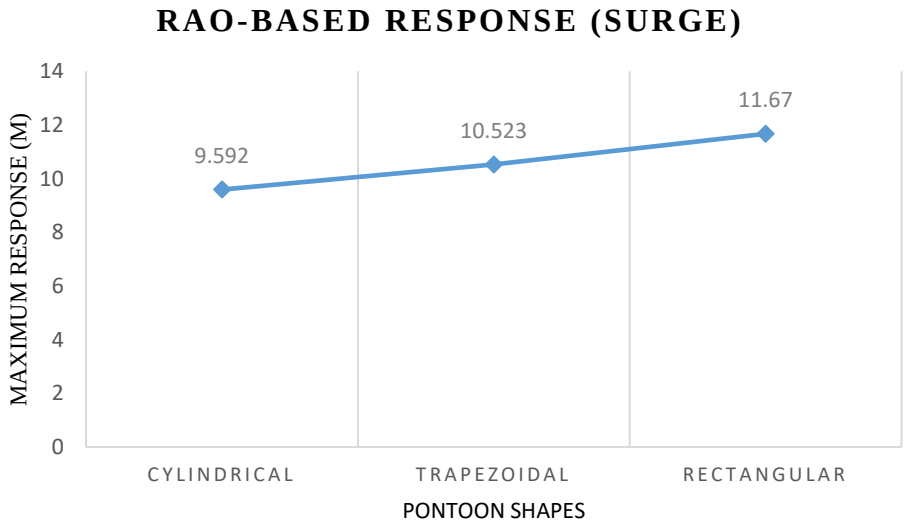

FIGURE 4.8: Maximum response for surge

4.2.3 Heave Response for Airy Wave

Figures 4.9, 4.10, and 4.11 depicted the **RAO-based response** heave for each different model under the Airy Wave Theory.

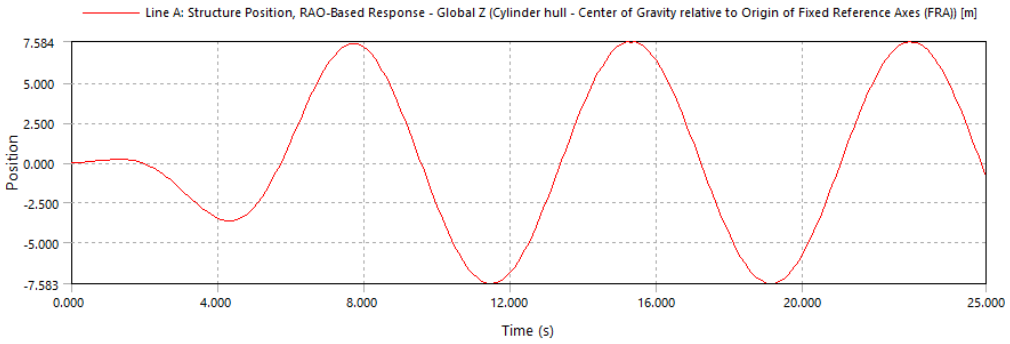

FIGURE 4.9: Airy wave heave response for cylindrical pontoon

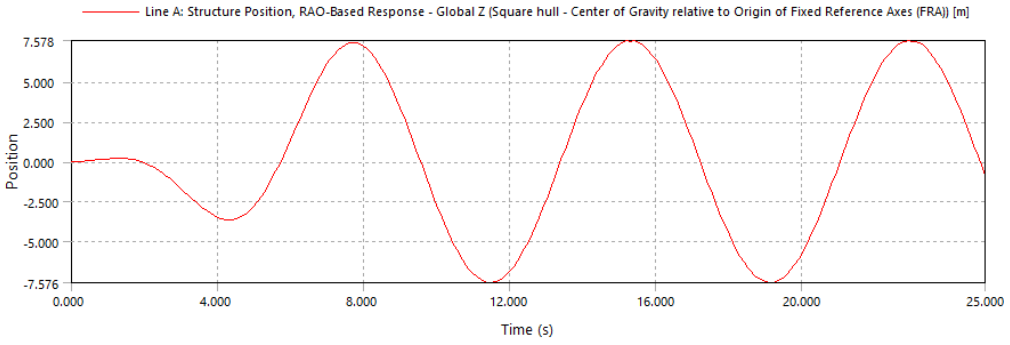

FIGURE 4.10: Airy wave heave response for rectangular pontoon

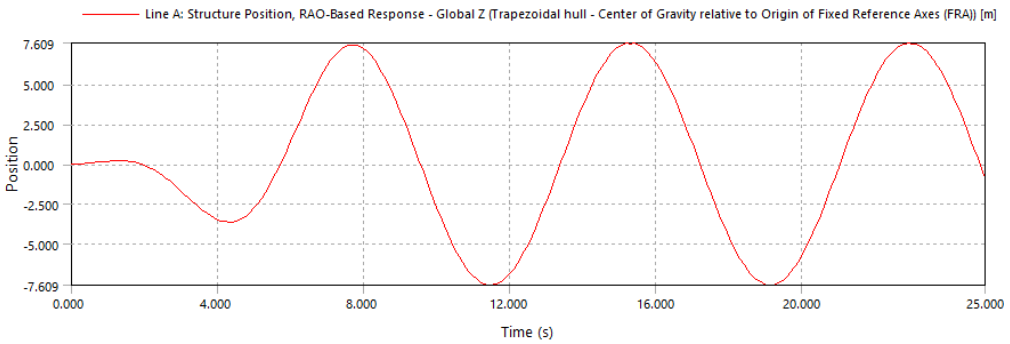

FIGURE 4.11: Airy wave heave response for trapezoidal pontoon

Figure 4.12 represents the impact of heave response on the pontoon shapes of the floating solar unit. The maximum response for heave is the trapezoidal pontoon which is 7.609 m, followed by the cylindrical pontoon at 7.584 m and the rectangular pontoon at 7.578 m. When comparing the three models, it is clear that the trapezoidal pontoon has the largest maximum response and the rectangular pontoon has the best heave response since it has the smallest response.

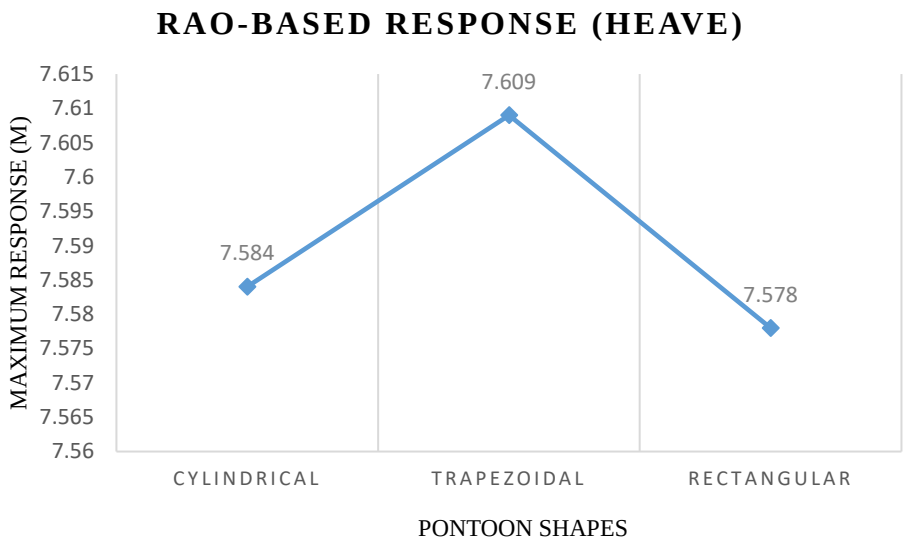

FIGURE 4.12: Maximum response for heave

4.2.4 Heave Response for Stokes 2nd Order

Figures 4.13, 4.14, and 4.15 show the characteristic of **RAO-based response** heave for different pontoons when subjected to Stokes 2nd Order wave Theory.

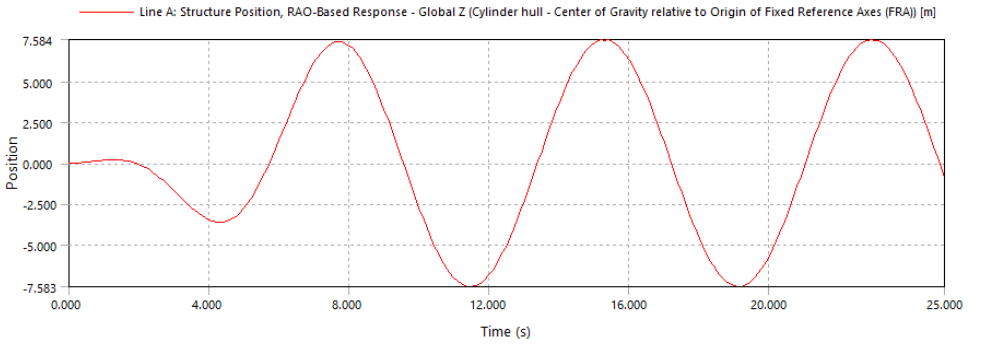

FIGURE 4.13: Stokes 2nd Order wave heave response for cylindrical pontoon

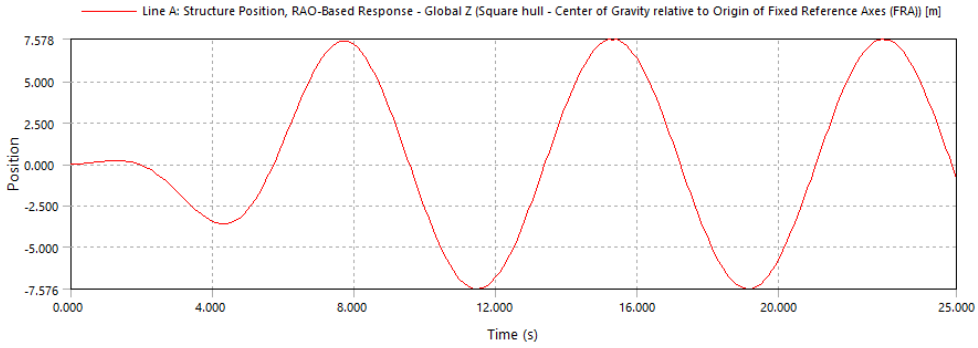

FIGURE 4.14: Stokes 2nd Order wave heave response for rectangular pontoon

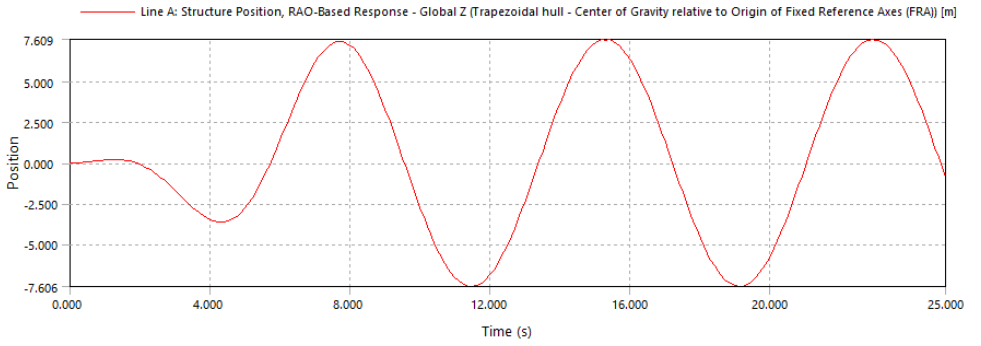

FIGURE 4.15: Stokes 2nd Order wave heave response for trapezoidal pontoon

Figure 4.16 represents the impact of heave response on the pontoon shapes of the floating solar unit. The maximum response for heave is the trapezoidal pontoon which is 7.609 m, followed by the cylindrical pontoon at 7.584 m and the rectangular pontoon at 7.578 m. When comparing the three models, it is clear that the trapezoidal pontoon has the largest maximum response and the rectangular pontoon has the best heave response since it has the smallest response. From the Airy wave and Stokes 2nd Order wave, both waves show that rectangular pontoon is the optimal design for floating solar farms to withstand heave response.

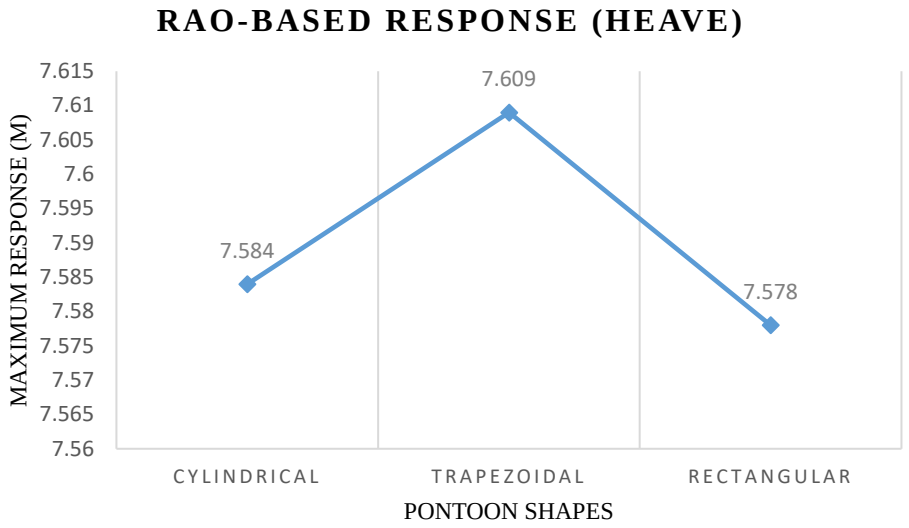

FIGURE 4.16: Maximum response for heave

4.2.5 Pitch Response for Airy Wave

Figures 4.17, 4.18, and 4.19 depicted the **RAO-based response** pitch for each different model under the Airy Wave Theory.

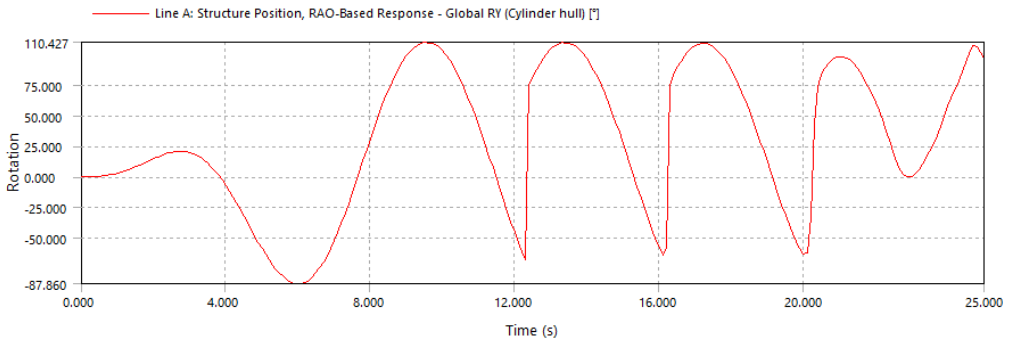

FIGURE 4.17: Airy wave pitch response for cylindrical pontoon

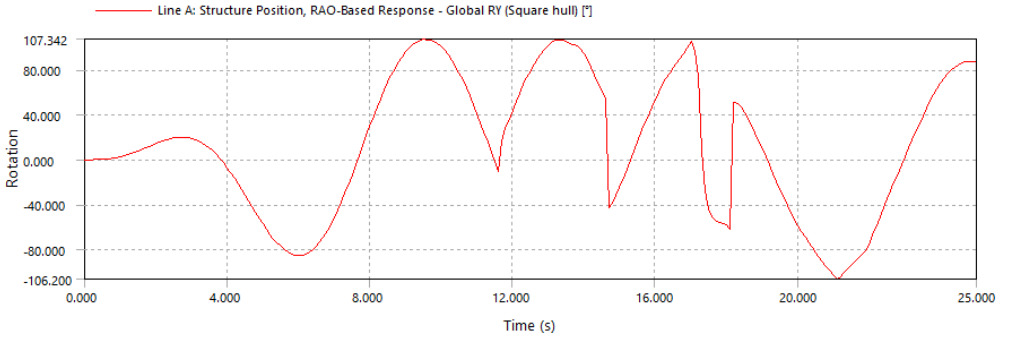

FIGURE 4.18: Airy wave pitch response for rectangular pontoon

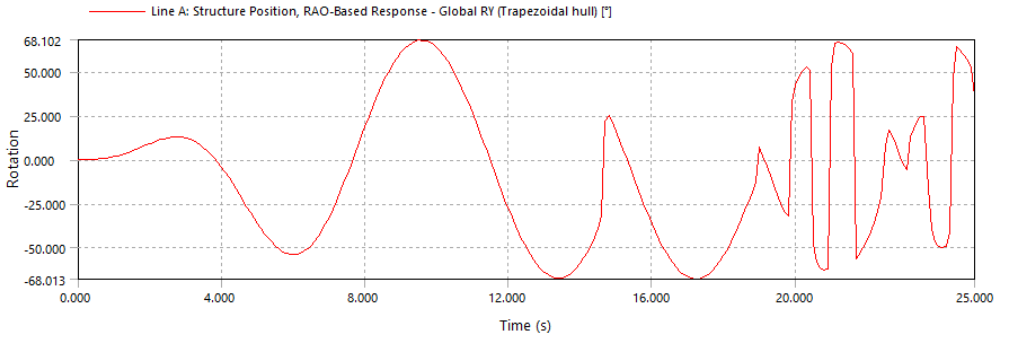

FIGURE 4.19: Airy wave pitch response for trapezoidal pontoon

Figure 4.20 represents the impact of pitch response on the pontoon shapes of the floating solar unit. The maximum response for pitch is the cylindrical pontoon which is 110.427°, followed by the rectangular pontoon at 107.342° and the trapezoidal pontoon at 68.102°. When comparing the three models, it is clear that the cylindrical pontoon has the largest maximum response and the trapezoidal pontoon has the best pitch response since it has the smallest response.

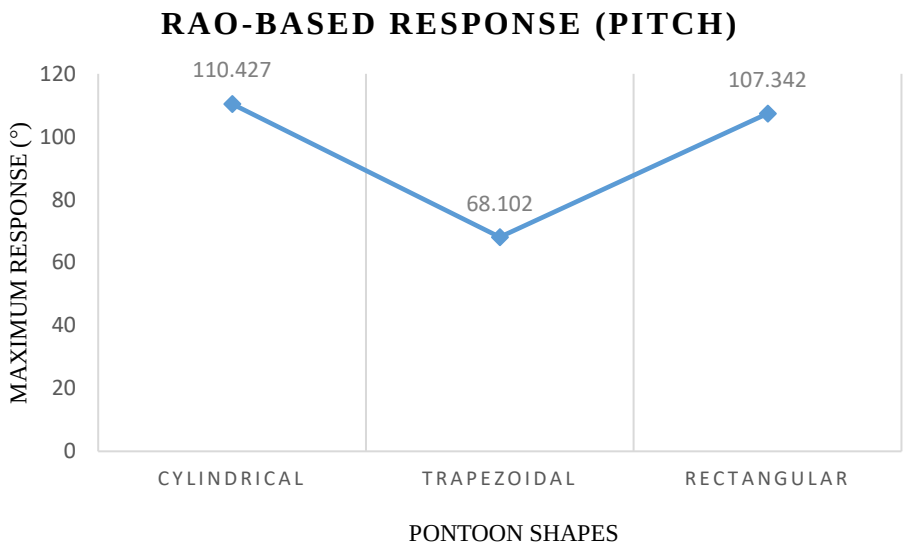

FIGURE 4.20: Maximum response for pitch

4.2.6 Pitch Response for Stokes 2nd Order

Figures 4.21, 4.22, and 4.23 show the characteristic of **RAO-based response** pitches for different pontoons when subjected to Stokes 2nd Order wave Theory.

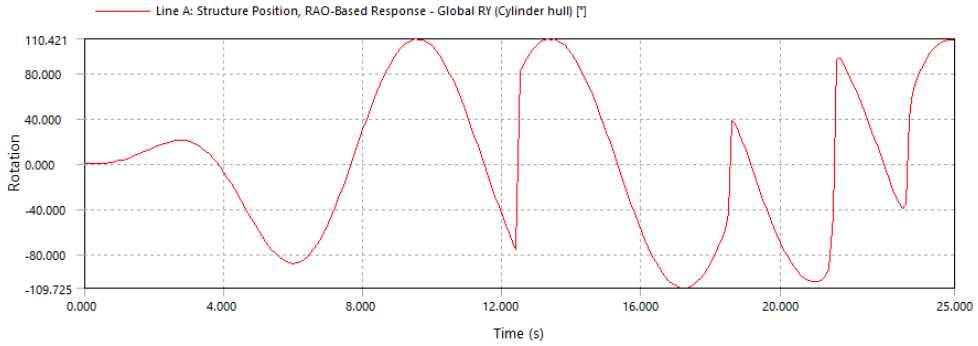

FIGURE 4.21: Stokes 2nd Order wave pitch response for cylindrical pontoon

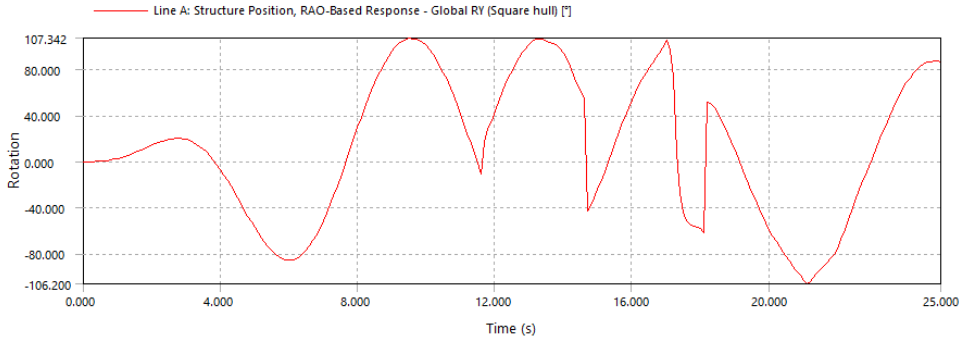

FIGURE 4.22: Stokes 2nd Order wave pitch response for rectangular pontoon

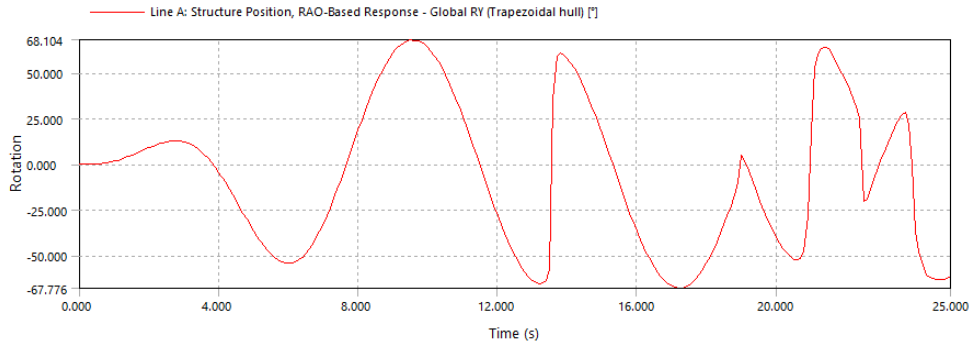

FIGURE 4.23: Stokes 2nd Order wave pitch response for trapezoidal pontoon

Figure 4.24 represents the impact of pitch response on the pontoon shapes of the floating solar unit. The maximum response for pitch is the cylindrical pontoon which is 110.421°, followed by the rectangular pontoon at 107.342° and the trapezoidal pontoon at 68.104°. When comparing the three models, it is clear that the cylindrical pontoon has the largest maximum response and the trapezoidal pontoon has the best pitch response since it has the smallest response. From Airy wave and Stokes 2nd Order wave, both waves show that trapezoidal pontoon is the optimal design for floating solar farms to withstand pitch response.

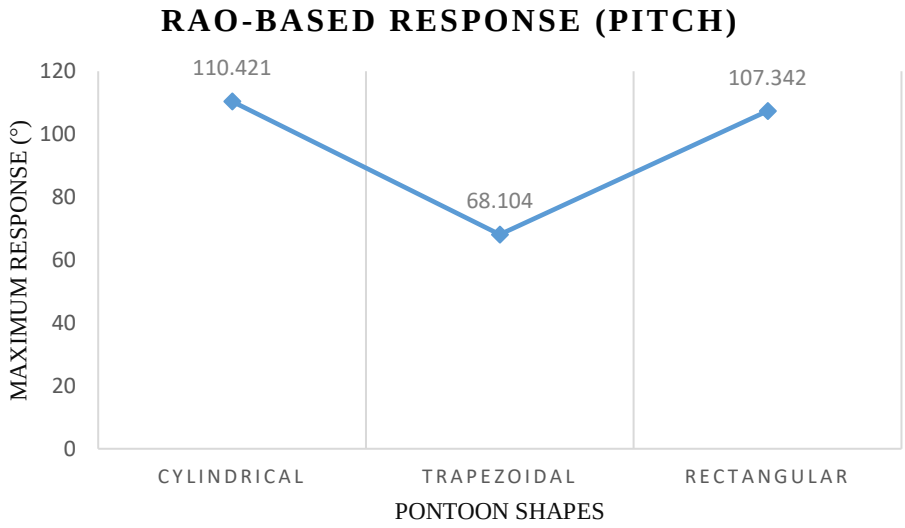

FIGURE 4.24: Maximum response for pitch

4.2.7 Maximum Response on Different Models on Regular Waves

TABLE 4.1: Maximum response for surge, heave, and pitch

Model	Surge	Heave	Pitch
Airy Wave Theory			
Cylindrical	9.593	7.584	110.427
Trapezoidal	10.523	7.609	68.102
Rectangular	11.67	7.578	107.342
Stokes 2nd Order			
Cylindrical	9.592	7.584	110.421
Trapezoidal	10.523	7.609	68.104
Rectangular	11.67	7.578	107.342

Table 4.1 indicates that Airy wave and Stokes 2nd Order wave share the same principles regarding the effects of pontoon shapes for the surge, heave, and pitch response. At surge, the cylindrical pontoon design is the most effective at withstanding the biggest response. However, rectangular pontoons outperform all other types of pontoons when it comes to heaving response. In terms of rotation pitch, trapezoidal pontoons have excellent performance in terms of overcoming rotation, it is essential to identify the optimum shapes so it can withstand wave motions. According to (Diendorfer, Haider, & Lauermann, 2014) avoiding platform motion is critical for cost-effective platform design, as even minor misalignments reduce solar collector efficiency. So a platform design was created that has minimal wave response. Theoretically, wave motion and direction affect performance.

4.3 Effects of Wave Types

4.3.1 RAO Response in Regular Wave

Figures 4.25, 4.26, and 4.27 illustrate the results of the RAO for the Airy wave and the Stokes 2nd Order wave at the surge, heave, and pitch responses, respectively.

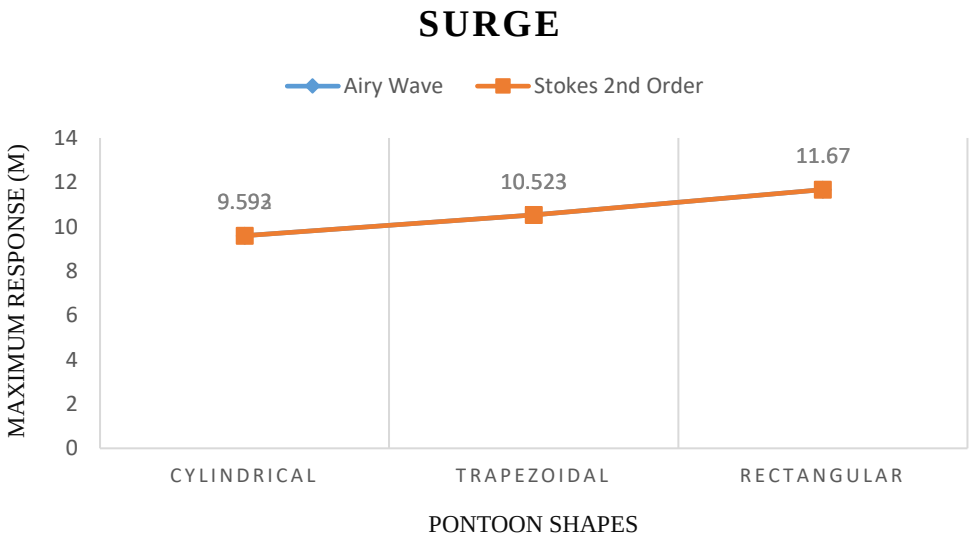

FIGURE 4.25: Surge response in regular wave

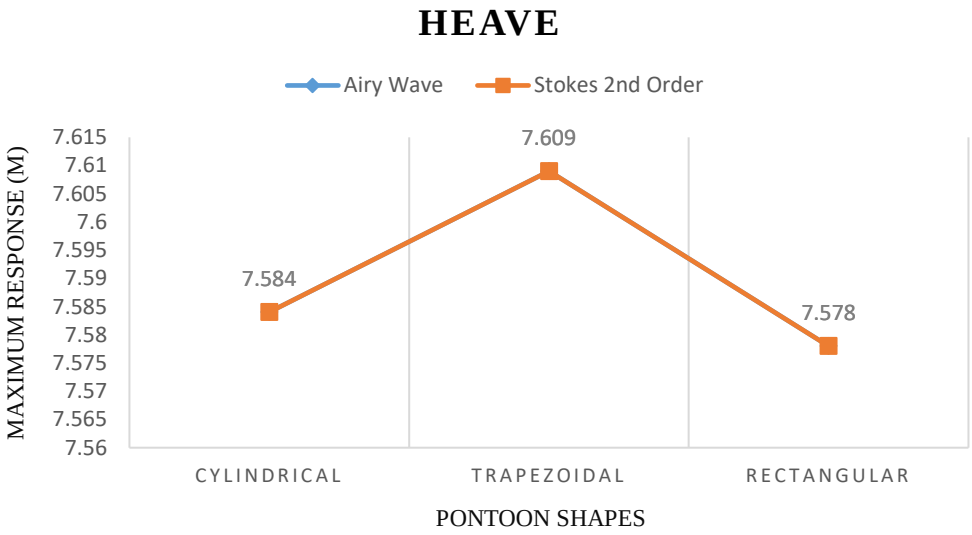

FIGURE 4.26: Heave response in regular wave

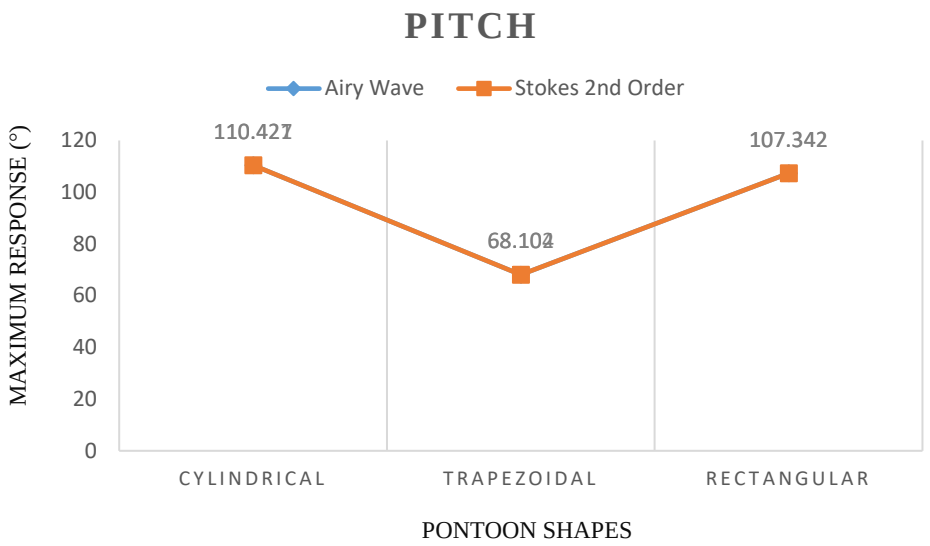

FIGURE 4.27: Pitch response in regular wave

Table 4.2 demonstrates that the response values for both waves are the same for each degree of freedom (DOF). **Figures 4.25, 4.26, and 4.27** display the same pattern for both waves as the graph shown in **Figure 4.25**. The difference between the RAO values for the two waves is extremely small, and a graph pattern develops between the two waves.

TABLE 4.2: Maximum response for surge, heave, and pitch

Model	Surge (m)	Heave (m)	Pitch (°)
Airy Wave Theory			
Cylindrical	9.593	7.584	110.427
Trapezoidal	10.523	7.609	68.102
Rectangular	11.67	7.578	107.342
Stokes 2nd Order			
Cylindrical	9.592	7.584	110.421
Trapezoidal	10.523	7.609	68.104
Rectangular	11.67	7.578	107.342

4.3.2 RAO Response in Irregular Wave

The RAO results for the JONSWAP Spectrum and the PM Spectrum for the surge, heave, and pitch responses are shown in **Figures 4.28, 4.29, and 4.30**, respectively.

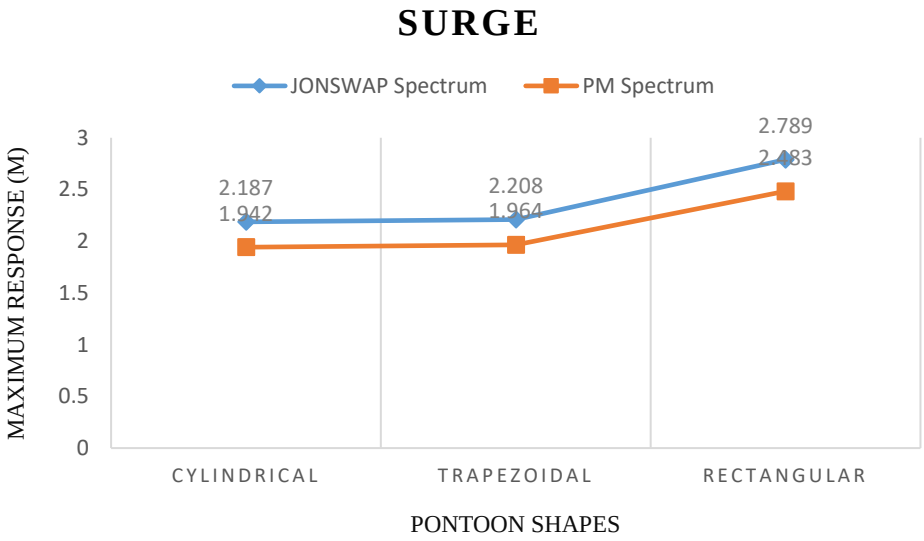

FIGURE 4.28: Surge response in irregular wave

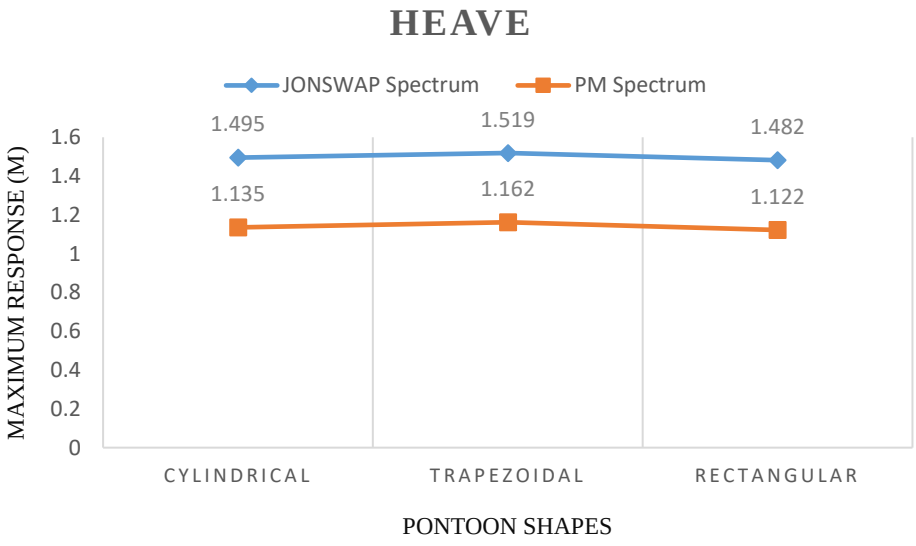

FIGURE 4.29: Heave response in irregular wave

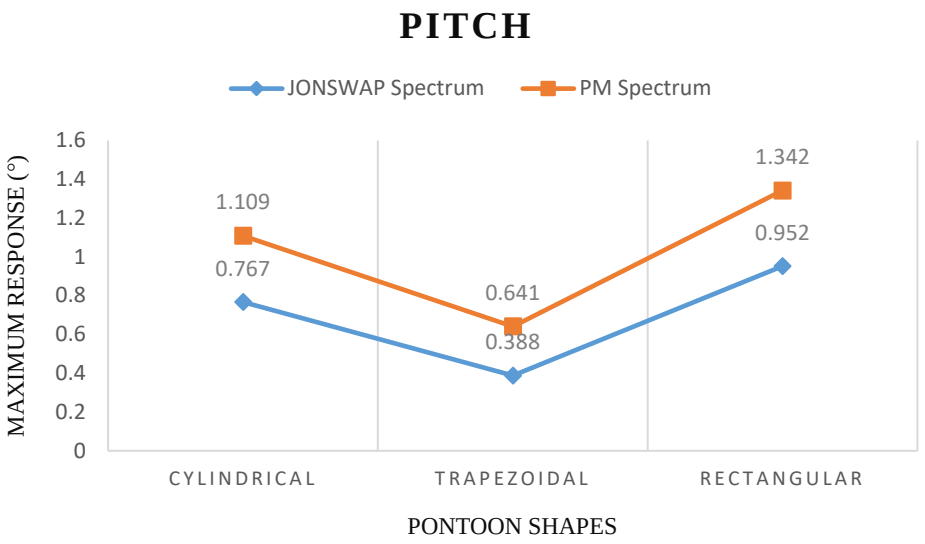

FIGURE 4.30: Pitch response in irregular wave

When irregular waves occur, the RAO reaction behaves differently than when regular waves occur. JONSWAP Spectrum has higher responsiveness than PM Spectrum when it comes to the degree of freedom (DOF) of the surge and heave as shown in **Table 4.3**. While at the pitch, PM Spectrum has more tendency to rotate since it has more response than JONSWAP Spectrum.

TABLE 4.3: Maximum response for surge, heave, and pitch

Model	Surge (m)	Heave (m)	Pitch (°)
JONSWAP Spectrum			
Cylindrical	2.187	1.495	0.767
Trapezoidal	2.208	1.519	0.388
Rectangular	2.789	1.482	0.952
PM Spectrum			
Cylindrical	1.942	1.135	1.109
Trapezoidal	1.964	1.162	0.641
Rectangular	2.483	1.122	1.342

4.4 Effects of Wave Direction

Tests were carried out on floating solar farms with rectangular pontoon shapes in different wave directions to observe the RAO response in the Airy wave and Stokes 2nd Order waves, respectively. In this study, the results were compared for three different wave directions, which were 0, 45, and 135 degrees, respectively. The result is stated in **Tables 4.4 and 4.5**.

Figure **4.31, 4.32 and 4.34** illustrates the date obtain from table 4.4 and 4.5

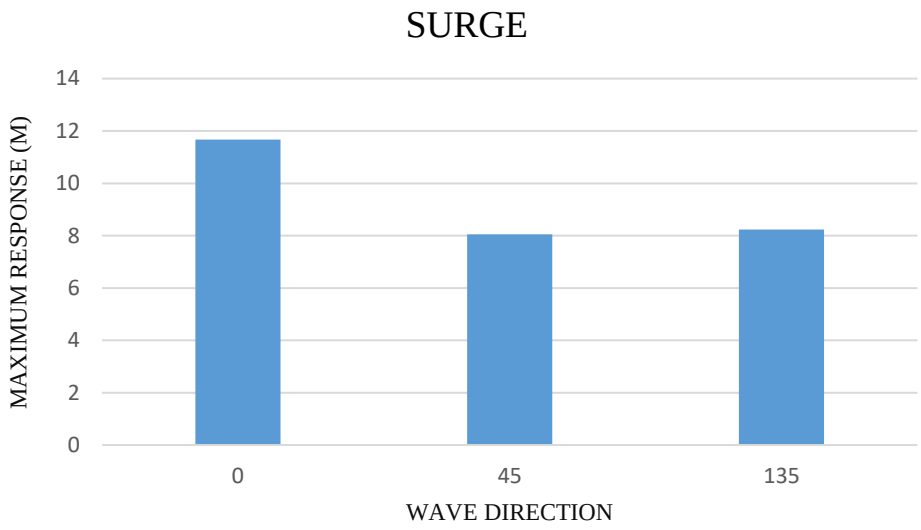

FIGURE 4.31: Surge response at wave direction

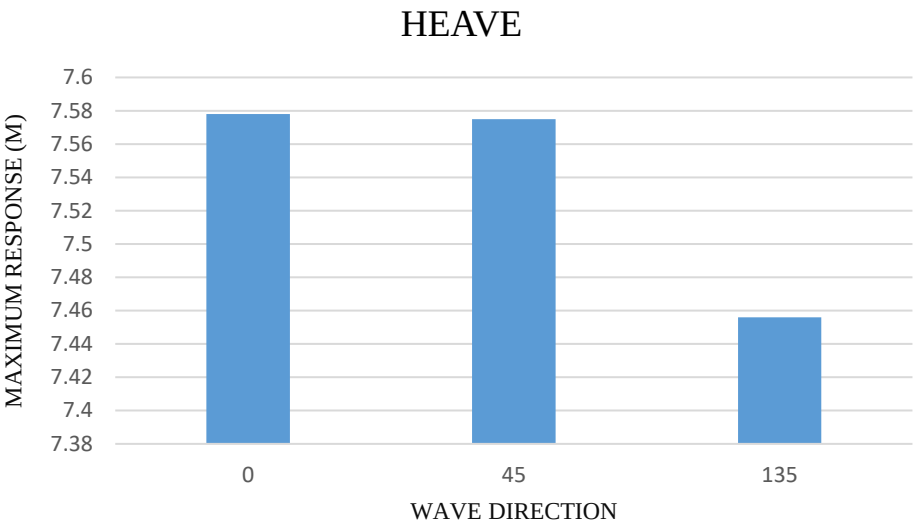

FIGURE 4.32: Heave response for different wave direction

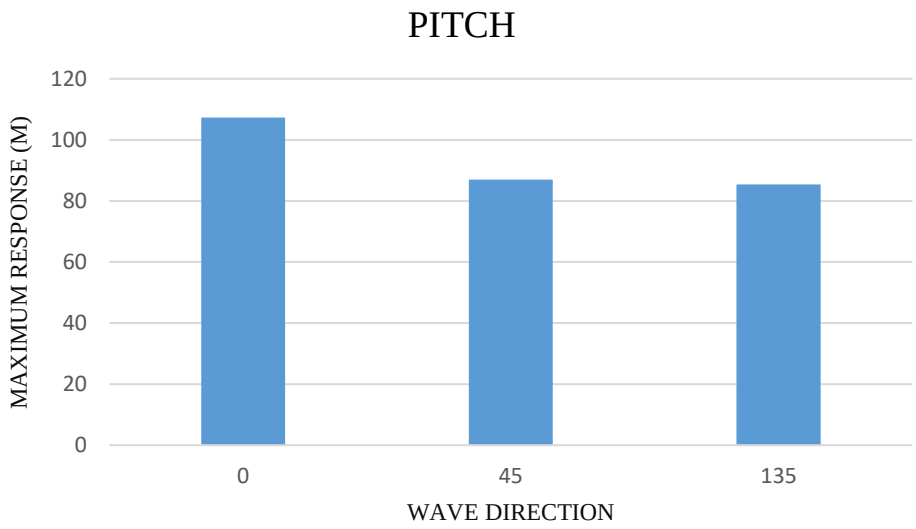

FIGURE 4.33: Pitch response at wave direction

RAO's critical response from three different wave orientations is shown in **Figures 4.31, 4.32, and 4.34**. For both an Airy and Stokes 2nd Order wave, surge at 0 degrees exhibits the largest surge response compared to 45 and 135 degrees of wave direction. Heave at 0 degrees also produced the strongest RAO reaction when compared to 45 and 135 degrees, and this was also true for Stokes 2nd Order. Lastly, rotation pitch at 0 degrees recorded the highest amount of response than 45 and 135 degrees of wave direction, which corresponded to the Stokes second-order wave.

TABLE 4.4: Wave direction in Airy Wave

Airy Wave Theory			
Wave direction (°)	**Surge (m)**	**Heave (m)**	**Pitch (°)**
0	11.67	7.578	107.342
45	8.056	7.575	86.941
135	8.231	7.456	85.361

TABLE 4.5: Wave direction in Stokes 2nd Order

Stokes 2nd Order			
Wave direction (°)	**Surge (m)**	**Heave (m)**	**Pitch (°)**
0	11.67	7.578	107.342
45	8.056	7.575	86.941
135	8.231	7.456	85.361

CHAPTER 5
CONCLUSION AND RECOMMENDATION

5.1 Conclusion

This paper aims to test various types of pontoon shapes against the wave and current loading to observe the dynamic response for each type of pontoon shape and its optimum shapes of pontoon. The methodology approach of this research is through finite element analysis and simulation using ANSYS and ANSYS AQWA. Results from the experiments is:

1. At surge, the cylindrical pontoon design is the most effective at withstanding the biggest response.
2. Rectangular pontoons outperform all other types of pontoons when it comes to heaving response.
3. At rotation pitch, trapezoidal pontoons have excellent performance in terms of overcoming rotation.
4. Stokes 2nd order and Airy wave share the same principle in term of RAO response.
5. JONSWAP spectrum have higher response at surge and heave than PM Spectrum
6. PM spectrum have higher response than JONSWAP spectrum at pitch.
7. 0 degree wave direction have the highest RAO response than 45 and 135 degrees.

5.2 Recommendation

Recommendation for this research on the dynamic analysis of floating solar unit subjected to second-order waves & current loadings is:

1) Perform a hydrodynamic response analysis using Design Modeller with different shapes of platform and mesh
2) Used new submerged floating photovoltaic PV system.
3) Changing wave height and wall thickness

REFERENCES

Bei, Y., Yuan, B., Yu, Y., Zhu, L., & Cao, D. (2021). Numerical analysis report on fluids in floating photovoltaic power plants. *Journal of Physics: Conference Series, 1985*(1). doi:10.1088/1742-6596/1985/1/012012

Cazzaniga, R., Cicu, M., Rosa-Clot, M., Rosa-Clot, P., Tina, G. M., & Ventura, C. (2018). Floating photovoltaic plants: Performance analysis and design solutions. *Renewable and Sustainable Energy Reviews, 81*, 1730-1741. doi:10.1016/j.rser.2017.05.269

Chakrabarti, S. K. (2005). *HANDBOOK OF OFFSHORE ENGINEERING* (Vol. 1). The Boulevard, Langford Lane, Kidlington, Oxford OX5 IGB, UK: Elsevier.

Cho, J.-R., Cho, Y.-U., Jeong, W.-B., Hong, S.-P., & Chun, H.-H. (2013). Dynamic Responses of Floating Platform for Spar-type Offshore Wind Turbine: Numerical and Experimental.

Choi, Y. R., Hong, S. Y., & Choi, H. S. (2000). An analysis of second-order wave forces on floating bodies by using a higher-order boundary element method. *Ocean Engineering, 28*, 117–138.

Diendorfer, C., Haider, M., & Lauermann, M. (2014). Performance Analysis of Offshore Solar Power Plants. *Energy Procedia, 49*, 2462-2471. doi:10.1016/j.egypro.2014.03.261

Friel, D., Karimirad, M., Whittaker, T., Doran, J., & Howlin, E. (2019). A review of floating photovoltaic design concepts and installed variations. *4th International Conference on Offshore Renewable Energy*.

Grainger, J. P., Sykulski, A. M., Jonathan, P., & Ewans, K. (2021). Estimating the parameters of ocean wave spectra. *Ocean Engineering, 229*. doi:10.1016/j.oceaneng.2021.108934

Ishihara, T., Phuc, P. V., & Sukegawa, H. (2007). A numerical study on the dynamic response of a floating offshore wind turbine system due to resonance and nonlinear wave.

Kaymak, M. K., & Şahin, A. D. (2021). Problems encountered with floating photovoltaic systems under real conditions: A new FPV concept and novel solutions. *Sustainable Energy Technologies and Assessments, 47*. doi:10.1016/j.seta.2021.101504

Kumar, M., Mohammed Niyaz, H., & Gupta, R. (2021). Challenges and opportunities towards the development of floating photovoltaic systems. *Solar Energy Materials and Solar Cells, 233*. doi:10.1016/j.solmat.2021.111408

Maâtoug, M. A., & Ayadi, M. (2016). Numerical simulation of the second-order Stokes theory using finite difference method. *Alexandria Engineering Journal, 55*(3), 3005-3013. doi:10.1016/j.aej.2016.04.035

Miao, Y.-j., Chen, X.-j., Ye, Y.-l., Ding, J., & Huang, H. (2021). Numerical modeling and dynamic analysis of a floating bridge subjected to wave, current and moving loads. *Ocean Engineering, 225*. doi:10.1016/j.oceaneng.2021.108810

Muhammad-Sukki, F., Munir, A. B., Ramirez-Iniguez, R., Abu-Bakar, S. H., Mohd Yasin, S. H., McMeekin, S. G., & Stewart, B. G. (2012). Solar photovoltaic in Malaysia: The way forward. *Renewable and Sustainable Energy Reviews, 16*(7), 5232-5244. doi:10.1016/j.rser.2012.05.002

Pa'suya, M. F., Omar, K. M., Peter, B. N., & Din, A. H. M. (2014). *Ocean surface circulation along peningsular Malaysia's Eastern Continental Shelf from nineteen years satellite altimetry data*. Paper presented at the 2014 IEEE 5th Control and System Graduate Research Colloquium.

Pimentel Da Silva, G. D., & Branco, D. A. C. (2018). Is floating photovoltaic better than conventional photovoltaic? Assessing environmental impacts. *Impact Assessment and Project Appraisal, 36*(5), 390-400. doi:10.1080/14615517.2018.1477498

Qu, X., Li, Y., Tang, Y., Hu, Z., Zhang, P., & Yin, T. (2020). Dynamic response of spar-type floating offshore wind turbine in freak wave considering the wave-current interaction effect. *Applied Ocean Research, 100*. doi:10.1016/j.apor.2020.102178

Ranjbaran, P., Yousefi, H., Gharehpetian, G. B., & Astaraei, F. R. (2019). A review on floating photovoltaic (FPV) power generation units. *Renewable and Sustainable Energy Reviews, 110*, 332-347. doi:10.1016/j.rser.2019.05.015

Sujay, S. P., Wagh, M. M., & Shinde, N. N. (2017). A Review on Floating Solar Photovoltaic Power Plants. *International Journal of Scientific & Engineering Research, 8*(6).

Zhang, Y., Jeng, D. S., Gao, F. P., & Zhang, J. S. (2013). An analytical solution for response of a porous seabed to combined wave and current loading. *Ocean Engineering, 57*, 240-247. doi:10.1016/j.oceaneng.2012.09.001

APPENDICES

APPENDIX 1

Unit	Derivation
x	the horizontal coordinate
z	the vertical coordinate, with the positive z-direction upward – opposing to the direction of the Earth's gravity – and $z = 0$ corresponding with the mean surface elevation
t	time
a	the first-order wave amplitude
k	the angular wavenumber, $k = 2\pi / \lambda$ with λ being the wavelength
ω	the angular frequency, $\omega = 2\pi / \tau$ where τ is the period
g	the strength of the Earth's gravity, a constant in this approximation.